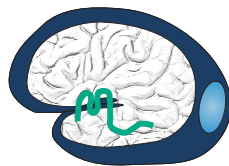


**SIGNALING PATHWAYS
ACTIVATED BY STRESS FACTORS
IN BRAIN ENDOTHELIAL CELLS**

Ph.D. Thesis

Imola Wilhelm

Supervisor: Dr. István A. Krizbai



Laboratory of Molecular Neurobiology

Institute of Biophysics

Biological Research Center

Hungarian Academy of Sciences

Szeged

-2009-

Publications related to the thesis:

I. Wilhelm I, Nagyószai P, Farkas AE, Couraud PO, Romero IA, Weksler B, Fazakas C, Dung NT, Bottka S, Bauer H, Bauer HC, Krizbai IA. Hyperosmotic stress induces Axl activation and cleavage in cerebral endothelial cells. *J Neurochem*. 2008, **107**:116-26. IF₂₀₀₇: 4.451

II. Wilhelm I, Farkas AE, Nagyószai P, Váró G, Bálint Z, Végh GA, Couraud PO, Romero IA, Weksler B, Krizbai IA. Regulation of cerebral endothelial cell morphology by extracellular calcium. *Phys Med Biol*. 2007, **52**:6261-74. IF₂₀₀₇: 2.528

Publications not directly related to the thesis:

1. Vajda S, Bartha K, **Wilhelm I**, Krizbai IA, Ádám-Vizi V. Identification of protease-activated receptor-4 (PAR-4) in puromycin-purified brain capillary endothelial cells cultured on Matrigel. *Neurochem Int*. 2008, **52**:1234-9. IF₂₀₀₇: 2.975

2. Hutamekalin P, Farkas AE, Orbók A, **Wilhelm I**, Nagyószai P, Veszélka S, Deli MA, Buzás K, Hunyadi-Gulyás E, Medzihradszky KF, Meksuriyen D, Krizbai IA. Effect of nicotine and polyaromatic hydrocarbons on cerebral endothelial cells. *Cell Biol Int*. 2008, **32**:198-209. IF₂₀₀₇: 1.547

3. Bálint Z, Krizbai IA, **Wilhelm I**, Farkas AE, Párducz A, Szegletes Z, Váró G. Changes induced by hyperosmotic mannitol in cerebral endothelial cells: an atomic force microscopic study. *Eur Biophys J*. 2007, **36**:113-20. IF₂₀₀₇: 2.238

4. Krizbai IA, Lenzser G, Szatmari E, Farkas AE, **Wilhelm I**, Fekete Z, Erdős B, Bauer H, Bauer HC, Sándor P, Komjáti K. Blood-brain barrier changes during compensated and decompensated hemorrhagic shock. *Shock*. 2005, **24**:428-33. IF₂₀₀₅: 3.122

5. Szabó H, Novák Z, Bauer H, Szatmári E, Farkas A, Wejksza K, Orbók A, **Wilhelm I**, Krizbai IA. Regulation of proteolytic activity induced by inflammatory stimuli in lung epithelial cells. *Cell Mol Biol (Noisy-le-grand)*. 2005, **51** Suppl:OL729-35. IF₂₀₀₅: 1.018

6. Farkas A, Szatmari E, Orbók A, **Wilhelm I**, Wejksza K, Nagyószai P, Hutamekalin P, Bauer H, Bauer HC, Traweger A, Krizbai IA. Hyperosmotic mannitol induces Src kinase-dependent phosphorylation of beta-catenin in cerebral endothelial cells. *J Neurosci Res*. 2005, **80**:855-61. IF₂₀₀₅: 3.239

ABBREVIATIONS:

Arp: actin-related protein
AJ: adherens junction
BBB: blood-brain barrier
bFGF: basic fibroblast growth factor
CEC: cerebral endothelial cell
CNS: central nervous system
EGF: epidermal growth factor
ERK: extracellular signal-regulated kinase
FAK: focal adhesion kinase
FBS: fetal bovine serum
FN: fibronectin
Gas6: growth arrest-specific protein 6
Gla: γ -carboxyglutamic acid
GTP: guanosine triphosphate
HRP: horseradish peroxidase
Ig: immunoglobulin
IP: immunoprecipitation
kDa: kilodalton
LG: laminin G
Ma: mannitol
MAP kinase: mitogen-activated protein kinase
MDCK: Madin-Darby canine kidney
PBS: phosphate-buffered saline
PDS: plasma derived serum
PDZ: post synaptic density protein (PSD95), *Drosophila* disc large tumor suppressor (DlgA), and zonula occludens-1 protein (ZO-1)
PI3K: Phosphoinositide 3-kinase
PKC: protein kinase C
PMA: phorbol 12-myristate 13-acetate
PY: phosphotyrosine
RTK: receptor tyrosine kinase
SDS: sodium dodecyl sulphate
SHBG: sex hormone-binding globulin
TBS: Tris-buffered saline
TJ: tight junction
Tris: tris(hydroxymethyl)aminomethane
ZO: zonula occludens

TABLE OF CONTENTS

1.	Introduction.....	6
1.1.	The blood-brain barrier.....	6
1.2.	The junctional complex	7
1.3.	Signaling at the tight junctions of brain endothelia.....	9
1.3.1.	Role of the Rho/Rho-kinase pathway.....	9
1.3.2.	Role of the phosphatidylinositol-3 kinase (PI3K)/Akt pathway	10
1.3.3.	Role of tyrosine phosphorylation and Axl.....	11
1.4.	Stress factor-induced changes in the brain endothelium	13
1.4.1.	Effect of depletion and readdition of extracellular calcium on the biogenesis of endothelial TJs.....	13
1.4.2.	Effects of hyperosmotic stress on CECs	14
2.	Material and methods.....	16
2.1.	Materials	16
2.2.	Cell culture	17
2.3.	Treatments	17
2.4.	Atomic force microscopy	18
2.5.	Immunofluorescence	18
2.6.	Detection of phosphoproteins using an antibody array	19
2.7.	Western-blot	19
2.8.	Immunoprecipitation	20
2.9.	Specific knockdown of Axl by RNA interference	21
2.10.	Real-time PCR.....	21
2.11.	Two-dimensional electrophoresis coupled with Western-blot	22
2.12.	Determination of apoptosis.....	22
3.	Results	23
3.1.	Role of Rho-kinase in the changes induced by calcium-switch	23

3.1.1.	Inhibition of Rho-kinase prevents morphological changes induced by calcium depletion	23
3.1.2.	Rho-kinase plays an important role in the calcium depletion-induced disassembly of endothelial tight and adherens junctions.....	25
3.1.3.	Cytoskeletal changes after calcium depletion are Rho-kinase dependent	25
3.2.	Effects of hyperosmotic stress.....	28
3.2.1.	Hyperosmotic stress induces activation of the Axl-Akt pathway	28
3.2.2.	Hyperosmosis induces degradation of Axl.....	30
3.2.3.	Phosphorylation and degradation of Axl are not directly related.....	34
3.2.4.	Axl is involved in the regulation (inhibition) of hyperosmotic mannitol-induced apoptosis.....	36
4.	Discussion.....	37
4.1.	Mechanisms regulating changes induced by calcium depletion and readdition....	37
4.2.	Hyperosmotic stress-induced Axl activation and cleavage	39
5.	Summary.....	43
6.	References	44
7.	Acknowledgements.....	51
8.	Appendix	52

1. INTRODUCTION

1.1. The blood-brain barrier

The blood–brain barrier (BBB) is a specialized system of endothelial cells lining brain microvessels, which shields the central nervous system (CNS) from potentially harmful and toxic substances of the blood, supplies brain tissues with nutrients, and removes metabolites from the brain back to the bloodstream. Therefore the blood-brain barrier has an important role in maintaining a precisely regulated microenvironment in the CNS. Endothelial cells are in a close interaction with other components of the neurovascular unit (pericytes, astrocytes and neurons) (Fig. 1) which induce and modulate the development and maintenance of the BBB characteristics of endothelial cells (for review see: Hawkins and Davis, 2005; Abbott *et al.*, 2006). Besides the BBB two more barrier layers limit and regulate molecular exchange at the interfaces between the blood and the neural tissue or its fluid spaces: the choroid plexus epithelium between blood and ventricular cerebrospinal fluid, and the arachnoid epithelium between blood and subarachnoid cerebrospinal fluid.

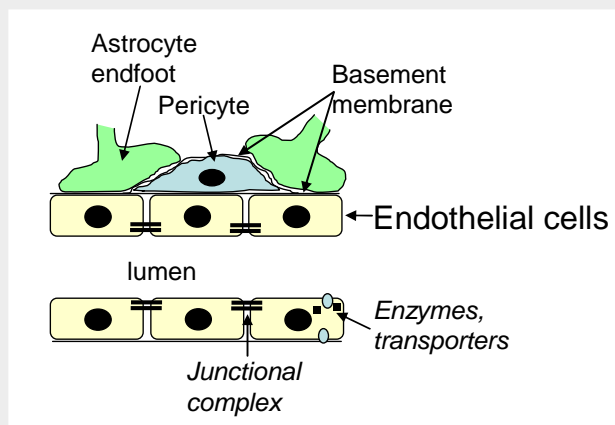


Fig. 1. Schematic representation of the neurovascular unit.

Transport across the BBB is strictly limited through a fourfold defense line: paracellular barrier (represented by interendothelial junctions); transcellular barrier (assured by the low level of endocytosis and transcytosis); enzymatic barrier (including acetylcholinesterase, alkaline phosphatase, γ -glutamyl transpeptidase, monoamine oxidases and drug metabolizing enzymes); and efflux transporters (ABC-B1, -C1, -C3, -C4, -C5, -C6, -G2). Small gaseous molecules such as O₂ and CO₂ can freely diffuse through the lipid membranes, and this is also a route of entry for small lipophilic agents, including barbiturates, nicotine and ethanol. However, specific blood-to-brain influx transport systems exist to supply nutrients like glucose, amino acids and nucleotides which cannot freely diffuse to the brain. Several independent carrier systems for the transport of hexoses (glucose, galactose), basic, acidic, and neutral amino acids, monocarboxylic acids (lactate, pyruvate, ketone bodies), purines (adenine, guanine), nucleosides (adenosine, guanosine, uridine), amines (choline), and ions have been described to be expressed in cerebral endothelial cells (CECs) (for review see: Abbott *et al.*, 2006; de Boer *et al.*, 2003).

From clinical point of view, BBB dysfunction plays an important role in the pathogenesis of many CNS diseases (HIV-1 encephalitis, Alzheimer's disease, ischemia, tumors, multiple sclerosis, and Parkinson's disease). On the other hand, as a result of restricted permeability, the BBB is a limiting factor for the delivery of therapeutic agents into the CNS (for review see: Persidsky *et al.*, 2006(b)).

1.2. The junctional complex

The junctional complex of CECs is formed by tight junctions (TJs) and adherens junctions (AJs).

Tight junctions of CECs act as a physical barrier forcing most molecular traffic to take a transcellular route across the BBB, rather than moving paracellularly through the junctions, as in most endothelia. Presence of a continuous line of tight junctions (Fig. 2) at cell-cell borders is one of the most important elements of the BBB phenotype of CECs. In this respect brain endothelial cells resemble epithelial cells. TJs are responsible for the separation of the apical and the basolateral membrane domain leading to the polarization of the cell ('fence function'), and for the restriction of the paracellular pathway ('gate function') (for review see: Gonzalez-Mariscal *et al.*, 2003).

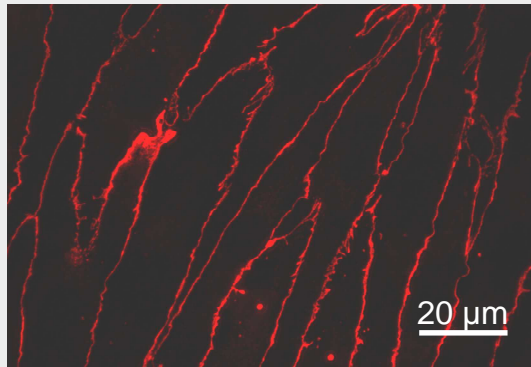


Fig. 2. Immunofluorescence staining of ZO-1 protein in cultured cerebral endothelial cells.

On transmission electron micrographs TJs appear as fusions of the plasma membrane between two cells ('kissing points') (Fig. 3). Intramembranous strands and complementary grooves can be visualized by freeze-fracture electron microscopy.

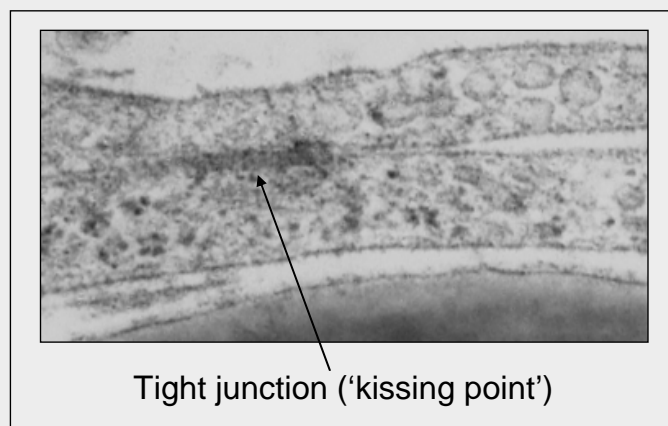


Fig. 3. Transmission electron microscopy image of tight junctions of brain endothelial cells.

The molecular components of the TJs can be separated into transmembrane and cytoplasmic plaque proteins. Transmembrane proteins of endothelial TJs include occludin (Furuse *et al.*, 1993), junctional adhesion molecules (Martin-Padura *et al.*, 1998) and members of the claudin family (Furuse *et al.*, 1998). Brain endothelial cells express claudin-5 (Morita *et al.*, 1999) and to a smaller extent claudin-3, 10, 12, and possibly other subtypes (Ohtsuki *et al.*, 2008). Plaque proteins link transmembrane proteins to the actin cytoskeleton and include PDZ-containing proteins, like zonula occludens (ZO)-1 (Stevenson *et al.*, 1986), ZO-2 (Gumbiner *et al.*, 1991)

and non-PDZ proteins like cingulin (Citi *et al.*, 1988 and 1989) or JACOP (junction-associated coiled-coil protein)/paracingulin (Ohnishi *et al.*, 2004).

AJs are ubiquitous in the vasculature and mediate adhesion of endothelial cells to each other, contact inhibition during vascular growth and remodeling, initiation of cell polarity, and – in part – regulation of paracellular permeability. The transmembrane proteins of the adherens junctions are the cadherins, in the case of vascular endothelial cells mainly VE-cadherin (Breier *et al.*, 1996), which is linked through the catenins (α , β and γ) to the cytoskeleton. A proper function of the adherens junction is needed for tight junction formation (Schulze and Firth, 1993). In addition, TJs and AJs may be even structurally interconnected, since it has been shown that ZO-1 and ZO-2 can interact with α -catenin (Itoh *et al.*, 1997 and 1999).

1.3. Signaling at the tight junctions of brain endothelia

Regulation of junctional proteins is under complex control. Expression and posttranslational modification of tight junctional proteins and regulation of paracellular permeability are precisely controlled and many signaling molecules proved to be localized to the junctions (for review see: Gonzalez-Mariscal *et al.*, 2008). Much of our knowledge concerning regulation of TJs arises from the study of epithelial cells, therefore specific regulation of the junctional complex of the BBB still remains to be elucidated (for review see: Krizbai and Deli, 2003). Among the most important signaling molecules involved in TJ regulation are cyclic nucleotides, Ca^{2+} , G-proteins, and members of signaling cascades based on serine/threonine and tyrosine phosphorylation (MAPKinases, Rho-kinase, tyrosine kinases, phosphatidylinositol-3 kinase (PI3K)/Akt). In our study we have focused on the role of Rho-kinase, the PI3K/Akt pathway and tyrosine phosphorylation mediated by the receptor tyrosine kinase Axl.

1.3.1. Role of the Rho/Rho-kinase pathway

Small guanosine triphosphate (GTP)-binding proteins provide a critical link between receptors at the cell surface and kinase cascades which regulate a variety of cellular processes. The Rho family of GTPases belongs to the Ras superfamily and includes RhoA, Rac and Cdc42. Downstream effectors of RhoA include the family of serine/threonine kinases termed p160ROCK (ROKb or ROCKI) and ROKa (ROCKII). Rho-kinases can induce acto-myosin contractility by

inducing phosphorylation of the regulatory myosin light chain (Hopkins *et al.*, 2003). Several plaque proteins of the TJ interact directly with actin. Such interactions stabilize the junctional complex at the cell border and also provide the force for the disruption of intercellular junctions upon contraction of the perijunctional acto-myosin ring. A balance between activity and quiescence of Rho GTPases appears crucial for both generation and maintenance of the optimal barrier function (Hopkins *et al.*, 2003).

In CECs activation of the Rho/Rho-kinase pathway in different pathological conditions leads to the disruption of the junctions. Rho and Rho-kinase have been shown to have a pivotal role in chemokine-induced junctional disarrangement (Stamatovic *et al.*, 2003 and 2006). It has also been shown that inhibition of the Rho pathway results in the upregulation of TJ proteins, prevents occludin and claudin-5 phosphorylation (induced by monocytes), and diminishes monocyte transendothelial migration (Persidsky *et al.*, 2006(a); Yamamoto *et al.*, 2008). Enhanced adhesion and migration of HIV-1 infected monocytes across the BBB were significantly reduced when Rac1 and RhoA inhibition was induced by a PPAR γ agonist (Ramirez *et al.*, 2008). RhoA activation is also involved in methamphetamine-, HIV gp120- and reactive oxygen species-induced TJ disruption (Mahajan *et al.*, 2008; Schreiber *et al.*, 2007) and in small cell lung cancer migration through brain microvascular endothelial cells (Li *et al.*, 2006).

1.3.2. Role of the phosphatidylinositol-3 kinase (PI3K)/Akt pathway

Phosphoinositide 3-kinases (PI3Ks) are enzymes capable of phosphorylating the third hydroxyl group of the inositol ring of phosphatidylinositol. Class I PI3Ks are composed of catalytic and regulatory subunits, respectively, known as p110 and p85. These kinases convert PI(4,5)P₂ to PI(3,4,5)P₃ on the inner leaflet of the plasma membrane. PI(3,4,5)P₃ induces translocation of Akt (protein kinase B, PKB), a serine/threonine kinase, from the cytosol to the cell membrane. In the membrane Akt becomes activated after being phosphorylated at threonine308 and serine473 by phosphoinositide-dependent kinase-1 and -2. Downstream targets of Akt include the glycogen synthase kinase, which is responsible for the degradation of β -catenin, through the ubiquitin proteasome pathway; snail, a transcription factor that inhibits the transcription of E-cadherin, occludin and claudins; and Bcl-2-associated death protein, which

blocks mitochondrial cytochrome c release and caspase activity. Akt is known to be involved in cell survival and proliferation.

In CECs the PI3K/Akt pathway mediates alterations of the endothelial barrier in response to different extracellular factors as well. Hypoxia and VEGF were shown to increase permeability through rearrangement of endothelial junctional proteins involving activation of the PI3K/Akt pathway (Fischer *et al.*, 2004; Vogel *et al.*, 2007) and this signaling route mediates reactive oxygen species-induced alteration of brain endothelial tight junction dynamics as well (Schreibelt *et al.*, 2007). HIV-1 Tat protein and focal cerebral ischemia were also shown to exert at least partially their BBB damaging effect through the PI3K/Akt pathway (András *et al.*, 2005; Kilic *et al.*, 2006). Furthermore, activation of the PI3K/Akt pathway was shown to have proangiogenic and cytoprotective effects in human brain microvascular endothelial cells and human umbilical vein endothelial cells (Lok *et al.*, 2008; Park *et al.*, 2008). Moreover, hypoxic preconditioning has been proved to protect the human brain endothelium from ischemic apoptosis through Akt-dependent survivin activation (Zhang *et al.*, 2007). These studies point to the pro-survival and anti-apoptotic role of Akt in CECs.

1.3.3. Role of tyrosine phosphorylation and Axl

Protein phosphorylation plays an important role in the cellular adaptation to diverse extracellular stimuli, and affects several types of proteins including signaling molecules, cytoskeletal elements, junctional proteins, etc. Phosphorylation of junctional proteins may occur on both tyrosine and serine/threonine residues and depending on the site of phosphorylation it may favor either TJ formation and decrease in permeability or loosening of the TJ barrier. Tyrosine phosphorylation is essential for junctional assembly (Meyer *et al.*, 2001), however, in case of mature TJs tyrosine phosphorylation induces loosening of the barrier (Staddon *et al.*, 1995).

Receptor tyrosine kinases (RTKs) are high affinity cell surface receptors for many growth factors, cytokines and hormones. They contain an extracellular ligand binding and an intracellular kinase domain. When the specific ligand binds to the extracellular domain of the RTK, its dimerization is triggered with other adjacent RTKs. Dimerization leads to a rapid activation of the protein's cytoplasmic kinase domain, the first substrate being the receptor itself. As a result

the activated receptor becomes autophosphorylated on multiple specific intracellular tyrosine residues, followed by phosphorylation and activation of other proteins leading to the initiation of signal transduction pathways (for review see: Hubbard, 2002).

Axl (also called ARK, UFO and Tyro7) is a member of a family of receptor tyrosine kinases that includes Mer and Sky. Its natural ligand is the vitamin K-dependent protein Gas6 (growth arrest-specific protein 6) (for review see: Hafizi and Dahlbäck 2006(a) and 2006(b)). This family of receptor tyrosine kinases is characterized by two immunoglobulin (Ig)-like and two fibronectin (FN) type III domains in the N-terminal region and a tyrosine kinase domain in the intracellular C-terminal region (Fig. 4). Gas6 has the same domain organization as protein S, namely an N-terminal region containing 11 γ -carboxyglutamic acid residues (Gla), a loop region, four epidermal growth factor (EGF)-like repeats, and a C-terminal sex hormone-binding globulin (SHBG)-like structure that is composed of two globular laminin G-like (LG) domains (Fig. 4).

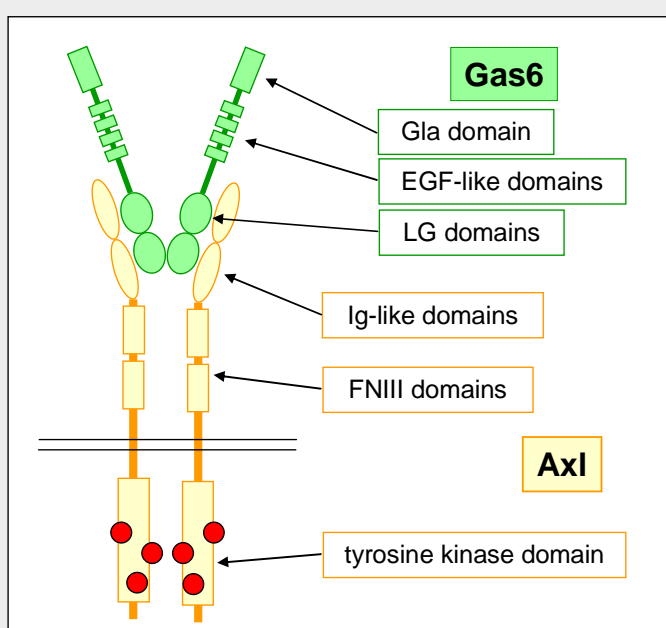


Fig. 4. Schematic representation of Axl and Gas6.

Axl has two alternatively spliced forms (O'Bryan *et al.*, 1995) that either contain or lack 9 amino acids carboxyl-terminal to the fibronectin domains in the extracellular part of the protein. Axl is emerging as a regulator of a large number of cellular functions and has been shown to be involved in the regulation of different aspects of endothelial function as well. It has been

demonstrated that activation of Axl can rescue endothelial cells from apoptosis (D'Arcangelo *et al.*, 2006; D'Arcangelo *et al.*, 2002; Hasanbasic *et al.*, 2004) and Axl is involved in cell migration and vascular remodeling (Korshunov *et al.*, 2007; Korshunov *et al.*, 2006) and angiogenesis (Gallicchio *et al.*, 2005; Holland *et al.*, 2005) as well. Activation of Axl results in its autocatalytic tyrosine phosphorylation, recruitment of different signaling molecules (Grb2 and the p85 subunit of phosphatidylinositol-3 kinase) (Weinger *et al.*, 2008) and activation of Akt and NF- κ B (Hasanbasic *et al.*, 2004). Besides its role in cell growth, survival and migration in vascular smooth muscle cells, endothelial cells and fibroblasts, Axl is a transforming gene enhancing cancer cell invasion (Holland *et al.*, 2005; Tai *et al.*, 2008).

1.4. Stress factor-induced changes in the brain endothelium

Endothelial cells are extremely important in sensing and responding to stress factors, contributing this way to the maintenance of brain homeostasis. These processes are regulated by a complex network of signaling pathways involving an impressive number of second messengers and protein kinases. Endothelial cells may become exposed to a series of different stress factors depending on the physiological or pathological condition involved, including shear-stress, oxidative stress, osmotic stress, changes in pH, ion or glucose concentration, etc. Being in close contact with the blood, endothelial cells are primarily exposed to stress factors and as a response they activate different signaling pathways.

1.4.1. Effect of depletion and readdition of extracellular Ca^{2+} on the biogenesis of endothelial TJs

Extracellular Ca^{2+} plays a crucial role in the formation and proper function of tight and adherens junctions (Gonzalez-Mariscal *et al.*, 1990; Pitelka *et al.*, 1983; Rothen-Rutishauser *et al.*, 2002). Ca^{2+} -switch experiments (i.e. depletion and subsequent readdition of extracellular Ca^{2+}) have been used to study the biogenesis of the junctions. However, the majority of data refer to epithelial junctions. It has to be mentioned that the molecular composition of epithelial and endothelial junctions is similar, however, not identical. For example, in endothelial cells the most important claudin is claudin-5, while in Madin-Darby canine kidney (MDCK) epithelial cells claudin-1, -3 and -4 are expressed at the highest levels. Moreover, the physical appearance of the

contact zone is different. In epithelial monolayers the cells attach to each other one by one like the bricks in a wall, while endothelial cells form plasma membrane folds at the contact sides, visible both by electron microscopy (Fig. 3) and atomic force microscopy. Therefore differences in Ca^{2+} depletion-induced changes might occur as well. Moreover, the mechanism of Ca^{2+} depletion-induced tight junction disassembly is still unclear.

1.4.2. Effects of hyperosmotic stress on CECs

It is well known that due to the relative impermeability of the BBB many drugs are unable to reach the CNS in therapeutically relevant concentration, making the BBB one of the major impediments in the treatment of CNS disorders. A large number of strategies have been developed in order to circumvent this problem. One of the successfully used methods to deliver drugs — especially antitumoral agents — to the CNS is the osmotic opening of the BBB using mannitol (for review see: Kroll and Neuwelt 1998; Rapoport, 2001). This causes a rapid opening (within minutes) of the BBB which is reversible. The barrier function starts to recover approximately 1 h after treatment, but complete recovery is achieved only after 6-8 h (Siegal *et al.*, 2000).

Hyperosmotic stress induces a variety of compensatory and adaptive responses in different cell types (for review see: Burg *et al.*, 2007). Hypertonicity can initiate a rapid reorganization of the actin cytoskeleton and promote association of cortactin with the actin-related protein 2/3 (Arp2/3) complex Di Ciano *et al.* (2002). Further research has revealed activation of Rho, Rac and Cdc42 as well (Di Ciano-Oliveira *et al.*, 2003; Lewis *et al.*, 2002). Our atomic force microscopic studies have revealed a significant decrease in cell height and elasticity accompanied by the appearance of cytoplasmic protrusions (Bálint *et al.*, 2007).

There is increasing evidence that hypertonicity induces a concerted action of signaling events. In this respect protein phosphorylation plays an important role in the cellular adaptation to hyperosmotic conditions and cellular shrinkage. It has been shown that a target of phosphorylation is cortactin, an actin-binding protein which is phosphorylated in a Fyn-dependent manner in Chinese hamster ovary cells (Kapus *et al.*, 1999). Another target protein of hyperosmotic stress-stimulated phosphorylation is focal adhesion kinase (FAK) which becomes phosphorylated on tyrosine397 and tyrosine577 via a Src-independent pathway in fibroblasts and

epithelial cells (Lunn *et al.*, 2004). However, less is known about endothelial, especially cerebral endothelial cells. In our previous study we have shown that hyperosmotic mannitol induces a rapid, concentration-dependent, and reversible tyrosine phosphorylation of a broad range of proteins between 50 and 190 kDa (Farkas *et al.*, 2005). A target of tyrosine phosphorylation is the adherens junction protein β -catenin, which after a Src kinase-dependent phosphorylation dissociates from the cadherin - α -catenin complex. However, other targets of hyperosmosis-induced tyrosine phosphorylation need to be identified.

Therefore, the **aim of our studies** was to identify new signaling pathways regulated by Ca^{2+} -switch and hyperosmosis in brain endothelial cells.

The following specific aims were addressed:

- 1a. Which are the molecular mechanisms regulating the morphological and cytoskeletal changes induced by Ca^{2+} depletion and readdition?
- 1b. Which mechanisms regulate the junctional changes induced by depletion and readdition of extracellular Ca^{2+} ?
- 2a. Which proteins are targets of tyrosine phosphorylation induced by hyperosmotic stress?
- 2b. What are the elements of the Axl signaling cascade activated by hyperosmosis?
- 2c. What are the mechanisms of Axl degradation?
- 2d. What is the role of osmotic stress-induced Axl activation?

2. MATERIAL AND METHODS

2.1. Materials

All chemicals, if not otherwise stated, were purchased from Sigma.

For isolation and culture of cells we have used: PDS (plasma derived serum) (First Link), FBS (fetal bovine serum), DMEM/F12 (Dulbecco's Modified Eagle Medium and Ham's F-12 Nutrient Mixture), MEM (Minimum Essential Medium), RPMI (Roswell Park Memorial Institute medium), collagenase type II, Percoll, puromycin (Sigma), EBM-2 (endothelial basal medium-2) and EGM-2 (endothelium growth medium-2) Bullet Kit (Cambrex), collagenase/dispase, bFGF (basic fibroblast growth factor) (Roche).

The following inhibitors and reagents were used: the tyrosine phosphatase inhibitor genistein, the Src-kinase inhibitor PP1 and the Rho-kinase inhibitor Y27632 (from Tocris), the metalloproteinase inhibitor GM6001, the calpain inhibitor calpeptin, the protein kinase C inhibitor bisindolylmaleinimide, the proteasome inhibitor MG132 and the caspase inhibitor zVAD (from Calbiochem). The 2,3-dimethoxy-1,4-naphthoquinone (DMNQ), the NF κ B inhibitor pyrrolidine dithiocarbamate (PDTC), sodium vanadate and verapamil were from Sigma. The protease inhibitors leupeptin, E64, pepstatin and pefabloc were from Roche, the ERK (extracellular signal-regulated kinase) inhibitor U0126 was bought from Cell Signaling and the PI3K inhibitor wortmannin was from Alomone.

We have used the following antibodies: rabbit anti-ZO-1, mouse anti-claudin-5 (Zymed), goat anti-Axl (C20) (Santa Cruz), rabbit anti-Akt, rabbit anti-phospho-Akt (Ser473), rabbit anti-cleaved caspase-3 (Asp175) (Cell Signaling), mouse anti-phosphotyrosine, mouse anti- β -actin, rabbit anti- β -catenin (Sigma), horseradish peroxidase (HRP)-anti-goat IgG (Santa Cruz), HRP-anti-mouse IgG (GE Healthcare), HRP-anti-rabbit IgG (Cell Signaling), Cy3-anti-goat IgG and -anti-rabbit IgG (Jackson). Alexa488-phalloidin was from Molecular Probes.

2.2. Cell culture

Primary rat brain endothelial cells were isolated from 2-week-old rats. Brains were cut into small pieces and digested in two steps with collagenase type II and collagenase/dispase, followed by centrifugation on Percoll gradient. The microvessel fragments were plated on rat tail collagen coated glass coverslips. The cells were cultured in DMEM/F12 medium containing 20% PDS, supplemented with 1 ng/ml bFGF and 100 µg/ml heparin at 37°C and 5% CO₂-containing atmosphere. In the first two days 4 µg/ml puromycin was added to remove contaminating cells (Perriere *et al.*, 2005). The cell layers reached confluency in 5-6 days and were used as primary cultures for the experiments.

Cell lines: The human endothelial cell line hCMEC/D3, obtained from Dr. P.O. Couraud (Paris, France), was maintained as described previously (Weksler *et al.*, 2005). Briefly, cells were grown on rat tail collagen coated plates or glass coverslips in EBM-2 medium supplemented with EGM-2 Bullet Kit and 2.5% FBS. Madin-Darby canine kidney (MDCK) cells were cultured in DMEM/F12 and 10% FBS. RG₂ rat glioma cells were cultured in RPMI and 10% FBS.

2.3. Treatments

All Ca²⁺ depletion and readdition experiments were carried out on confluent primary rat brain endothelial cells. After thorough wash in Ca²⁺-free PBS (phosphate-buffered saline), cells were kept in serum-free DMEM/F12 (Sigma D6421) (control) or MEM (Sigma M8167) (Ca²⁺ depletion) for 150 min. Recovery was performed in serum-free DMEM/F12 for 4 h. When indicated, the Rho-kinase inhibitor Y27632 was added at a concentration of 10 µM concomitantly with the Ca²⁺-free or recovery medium, respectively.

Hyperosmotic stress was elicited on confluent monolayers of hCMEC/D3 cells in serum-free culture medium using 10-20% mannitol (0.55-1.1 M, corresponding to an additional 550-1100 mOsmol/l compared to the 300 mOsmol/l control) for 10, 30 or 60 min. Various other substances were added concurrently with mannitol as indicated. Genistein treatment was performed with 1 h preincubation. Hyperosmosis was also elicited using 1.1 M arabinose or urea or 0.55 M NaCl in serum-free EBM-2 for 30 min. Effect of other stress factors were investigated using 10 µM DMNQ or 8 g/l glucose in serum-free EBM-2 for 30 min.

2.4. Atomic force microscopy

The atomic force microscope (AFM) invented by Binnig *et al.* (1986) allows the direct monitoring of spatial and temporal changes of the cell surface and submembranous structures at high resolution. Its main advantage is that in contrast to other high resolution techniques, i.e. electron microscopy, no fixation is needed, therefore living cells can be directly studied (Henderson *et al.*, 1992; Rotsch and Radmacher, 2000). The experiments were carried out within three hours from removing the cells from the thermostate at a temperature about 31°C. Consistently with literature data (Pesen and Hoh, 2005) during this period the cells preserved their viability.

Measurements were performed with an Asylum MFP-3D head and Molecular Force Probe 3D controller (Asylum Research). The driver program MFP-3D Xop was written in IGOR Pro software (Wavemetrics). Silicon nitride, rectangular cantilevers have been used with a typical spring constant of 0.03 N/m (Olympus, Optical Co. Ltd.). The cantilevers were silanized. The spring constant of the cantilevers was determined by thermal calibration. Typically 256x256 point scans were taken with a scan speed of 50 $\mu\text{m/s}$. The measurements were carried out in contact mode in fluid with an average loading force less than 1 nN. Both the trace and retrace images were measured and compared.

2.5. Immunofluorescence

Primary rat brain endothelial cells were cultured on rat tail collagen-coated glass coverslips and exposed to Ca^{2+} -switch. After the indicated treatments the cells were fixed using a mixture of ethanol:acetic acid (95:5) at -20°C for 10 min. Coverslips were washed in PBS and after blocking with 3% bovine serum albumin for 20 min, they were incubated with primary antibodies (rabbit anti-ZO-1 or mouse anti-claudin-5, diluted 1/200 in PBS containing 1% bovine serum albumin) for 90 min. After washing the staining was visualized using Cy2- or Cy3-conjugated secondary antibodies (diluted 1/400 in 1% bovine serum albumin-containing PBS, for 30 min, at room temperature). Coverslips were washed in PBS, rinsed in water. Mounting was performed in anti-fading embedding medium (Biomedica) and the distribution of the signal was studied using a Nikon Eclipse TE2000U photomicroscope with epifluorescent capabilities connected to a digital camera (Spot RT KE).

For phalloidin staining, cells were fixed with 4% formaldehyde, permeabilized using acetone at -20°C for 10 min. After blocking, coverslips were incubated for 1 h with Alexa488-phalloidin (diluted 1/100 in a buffer containing 60 mM PIPES, 25 mM HEPES, 10 mM EGTA, 2 mM MgCl₂, 140 mM NaCl) at room temperature. Washing and mounting was performed as previously described.

Axl staining was performed on hCMEC/D3 cells cultured on rat tail collagen-coated glass coverslips. Cells were fixed with ethanol:acetic acid (95:5) at -20°C for 10 min, washed with PBS. Non-specific binding sites were blocked with 3% bovine serum albumin for 20 min. The primary antibody was applied overnight at 4°C in 1/50 dilution. Cy-3 conjugated donkey anti-goat IgG (H+L) was used as secondary antibody diluted 1/100 for 30 min at room temperature.

2.6. Detection of phosphoproteins using an antibody array

The antibody array (Hypromatrix) contained antibodies against proteins of different signaling pathways. The antibodies were immobilized on a membrane, each at a predetermined position.

Cells were lysed in a buffer containing 20 mM Tris, 150 mM NaCl, 1 mM EDTA, 1% Triton X-100, 1 mM sodium vanadate, 10 mM NaF, 1 mM Pefabloc and centrifuged (10,000 x g, 10 min, 4°C). For blocking of nonspecific binding sites of the membrane 5% nonfat milk powder was used, diluted in TBS-T (Tris-buffered saline-Tween: 10 mM Tris-HCl (pH=7.4), 150 mM NaCl, 0.1% Tween 20). The cell homogenate was incubated with the antibody matrix for 2 h at room temperature with slow shaking. Following washing steps in TBS-T, the membrane was incubated with HRP-labelled anti-phosphotyrosine antibody (Hypromatrix) for 2 h. The membrane was washed and the reaction was visualized using enhanced chemiluminescence (ECL) Plus (GE Healthcare) on X-ray film (AGFA). Identity of phosphorylated proteins was determined from the position on the membrane.

2.7. Western-blot

Cells were washed with PBS and scraped into ice-cold lysis buffer (20 mM Tris, 150 mM NaCl, 1 mM EDTA, 1% Triton X-100, 1% sodium deoxycholate, 0.1% sodium dodecyl sulphate, 1 mM sodium vanadate, 10 mM NaF, 1 mM Pefabloc) and incubated on ice for 30 min. For

determination of water- and detergent soluble proteins the following buffers were used: 20 mM Tris, 150 mM NaCl, 1 mM EDTA, 1 mM sodium vanadate, 10 mM NaF, 1 mM Pefabloc for water-soluble proteins, and the same buffer containing 1% Triton X-100 for detergent-soluble proteins. Lysates were clarified by centrifugation at 10,000 x g for 10 min at 4°C and protein concentration was determined with the BCA method (Pierce).

Samples were prepared in Laemmli sample buffer (final concentration: 12 mM Tris-HCl (pH=6.8), 5% glycerol, 0.4% SDS (sodium dodecyl sulfate), 2.88 mM 2-mercaptoethanol, 0.02% bromophenol blue) and electrophoresed using standard denaturing SDS-PAGE (SDS polyacrylamide gel electrophoresis) procedures (electrophoresis buffer: 15.6 mM Tris, 120 mM glycine, 0.1% SDS) on 9% acrylamide gels.

Proteins were blotted onto PVDF (Pall) or nitrocellulose (Schleicher-Schuell) membranes (transfer buffer: 25 mM Tris, 194 mM glycine, 20% methanol). For blocking of nonspecific binding sites 5% nonfat milk powder or (in case of phospho-antibodies) 3% bovine serum albumin was used, diluted in TBS-T. Membranes were incubated with primary antibodies: anti-Axl (1/200), anti-phosphotyrosine (1/500) or anti- β -actin (1/1000) for 90 min. Anti-Akt and anti-pAkt antibodies were used in 1/500 dilution overnight at 4°C. Following washing steps in TBS-T, the membranes were incubated with the HRP-labelled secondary antibodies (1/5000) for 30 min. After repeated washing steps, the immunoreaction was visualized using ECL Plus chemiluminescence detection kit.

2.8. Immunoprecipitation

For immunoprecipitation experiments hCMEC/D3 were homogenized in lysis buffer as described above. Lysates were centrifuged at 10,000 x g for 10 min in a microfuge and the supernatant was used for immunoprecipitation. After preclearing with protein G Sepharose (GE Healthcare), 500 μ l supernatants with a total protein content of 0.5 mg were incubated with 2 or 5 μ g primary antibody (anti-Axl or -phosphotyrosine, respectively) at 4°C for 4 h. The formed immunocomplexes were precipitated by incubating the samples at 4°C overnight with protein G Sepharose beads. The precipitates were washed 4 times with lysis buffer, boiled in Laemmli sample buffer, and subjected to electrophoresis and immunoblotting.

2.9. Specific knockdown of Axl by RNA interference

StealthTM siRNA duplex oligoribonucleotides were designed using Invitrogen BLOCK-iTTM RNAi designer and were purchased from Invitrogen.

The sequences used were as follows:

sense, 5'-CAGGAACUGCAUGCUGAAUGAGAA-3';

antisense, 5'-UUCUCAUUCAGCAUGCAGUCCUGG-3'.

As control non-targeting RNA we have used the following scrambled oligonucleotides:

sense, 5'-GACGUAGAGAGAGUCCGACAACA-3';

antisense 5'-UGUAUGUCGGAACUCUCUCUACGUC-3'.

hCMEC/D3 cells were plated at 50% confluency in 3.5 cm diameter culture dishes. Transfection of oligonucleotides was then performed in OptiMEM medium containing 10 nM RNA and 5 μ l LipofectamineTM RNAiMAX reagent (Invitrogen). After 6 h the medium was changed to regular culture medium. In order to increase the efficiency, a second transfection was performed the following day. Cells were analyzed 24 h after the second transfection when they achieved confluency.

2.10. Real-time PCR

Total RNA was isolated using TRIzol reagent (Invitrogen). RNA was transcribed into cDNA using a reverse transcription kit (Fermentas). The amplification was performed on a BioRad iQ5 instrument using FastStart SYBR Green Mix (Roche) under the following conditions: 30 cycles of 95°C for 15 s, 55°C for 30 s, 72°C for 30 s.

The primer pairs used were the following:

GAS6: 5'-TGCTGTCATGAAAATCGCGG-3' and 5'-CATGTAGTCCAGGCTGTAGA-3',

Axl: 5'-GGTGGCTGTGAAGACGATGA-3' and 5'-CTCAGATACTCCATGCCACT-3',

GAPDH (glutaraldehyde-3-phosphate dehydrogenase) (used as control housekeeping gene): 5'-GTGAAGGTCGGTGTCAACG-3' and 5'-GTGAAGACGCCAGTAGACTC-3'.

Determination of threshold cycle and quantitation were performed using the software of the instrument.

2.11. Two-dimensional electrophoresis coupled with Western-blot

Control and mannitol treated cells were washed with Tris-buffered sorbitol (10 mM Tris, 25 mM sorbitol, pH=7.0) and scraped into sample-rehydration buffer (7 M urea, 2 M thiourea, 2% CHAPS, 1% DTT, 0.2 mM vanadate, 1 mM Pefabloc, 1 mM NaF, 0.2% ampholite, traces of bromophenol blue) and incubated at room temperature for 1 h. Debris was removed by centrifugation at 16,000 x g for 20 min on 17°C.

7 cm IPG (immobilized pH gradient) strips of linear pH gradient 4-7 (ReadyStrip, BioRad) were passively rehydrated for 16 h with 125 µl sample each. The isoelectric focusing (IEF) was carried out in a Protean IEF Cell (BioRad) using electrode wicks and oil covering. The IEF steps had the following parameters: 1: 250 V for 15 min, 2: 4,000 V for 3 h, 3: 17,000 Vh, 4: 500 V hold, voltage ramping was set to linear. The strips were equilibrated for 10 min in equilibrating buffer I (6 M urea, 4% SDS, 0.375 M Tris-HCl, 20% glycerol, 2% DTT) and for 10 min in equilibrating buffer II (6 M urea, 4% SDS, 0.375 M Tris-HCl, 20% glycerol, 2.5% iodoacetamide). The second dimension SDS-PAGE gel (10%) was run in a Mini-PROTEAN 3 Cell (BioRad). Western-blotting was performed on the second dimension gels.

2.12. Determination of apoptosis

Cells cultured on glass coverslips were transfected with Axl siRNA construct, followed by treatment with 20% mannitol for 3 h. In order to control the efficiency of silencing, parallel Western-blot analysis was performed using anti-Axl antibody. Immunofluorescence staining was done using anti-cleaved caspase-3 antibody. 1,000 cells/coverslip were analyzed under fluorescence microscope and labelled cells were counted. In another set of experiments nuclear morphology was analysed using Hoechst 33342 staining (0.6 µg/ml). Nuclei containing condensed chromatin at the nuclear envelope or fragmented chromatin were considered apoptotic (Bresgen *et al.*, 2003).

3. RESULTS

3.1. Role of Rho-kinase in the changes induced by Ca²⁺-switch

3.1.1. Inhibition of Rho-kinase prevents morphological changes induced by Ca²⁺ depletion

We were following the Ca²⁺ depletion- and readdition-induced morphological changes in living brain endothelial cells using atomic force microscopy. Confluent cultures of microvascular cerebral endothelial cells were exposed to Ca²⁺-switch, i.e. depletion and subsequent readdition of extracellular calcium ions.

After culturing the cells for 150 min in Ca²⁺-free medium we observed the appearance of interendothelial gaps (Fig. 5 d, f). The cells rounded up and the surface of the culture dish became visible. Detachment of the cells from each other was accompanied by a marked increase in the height of the cells (from about 1.5 μm to more than 3 μm at the highest point) (Fig. 5 b and e). The phenomenon was reversible: 1-2 h after readdition of the normal Ca²⁺ containing medium a disappearance of these changes was observed. The free surfaces were gradually occupied by the cells until total confluency was achieved. The initial height (above the nucleus approximately 1.5 μm) and shape was regained parallelly (Fig. 5 g, h, i).

We observed that addition of the Rho-kinase inhibitor Y27632 (10 μM) to the Ca²⁺-free medium prevented the appearance of morphological changes. No intercellular gaps were formed and the cells were closely attached to each other. The cells remained elongated and flattened and no increase in their height appeared (Fig. 5 j, k, l).

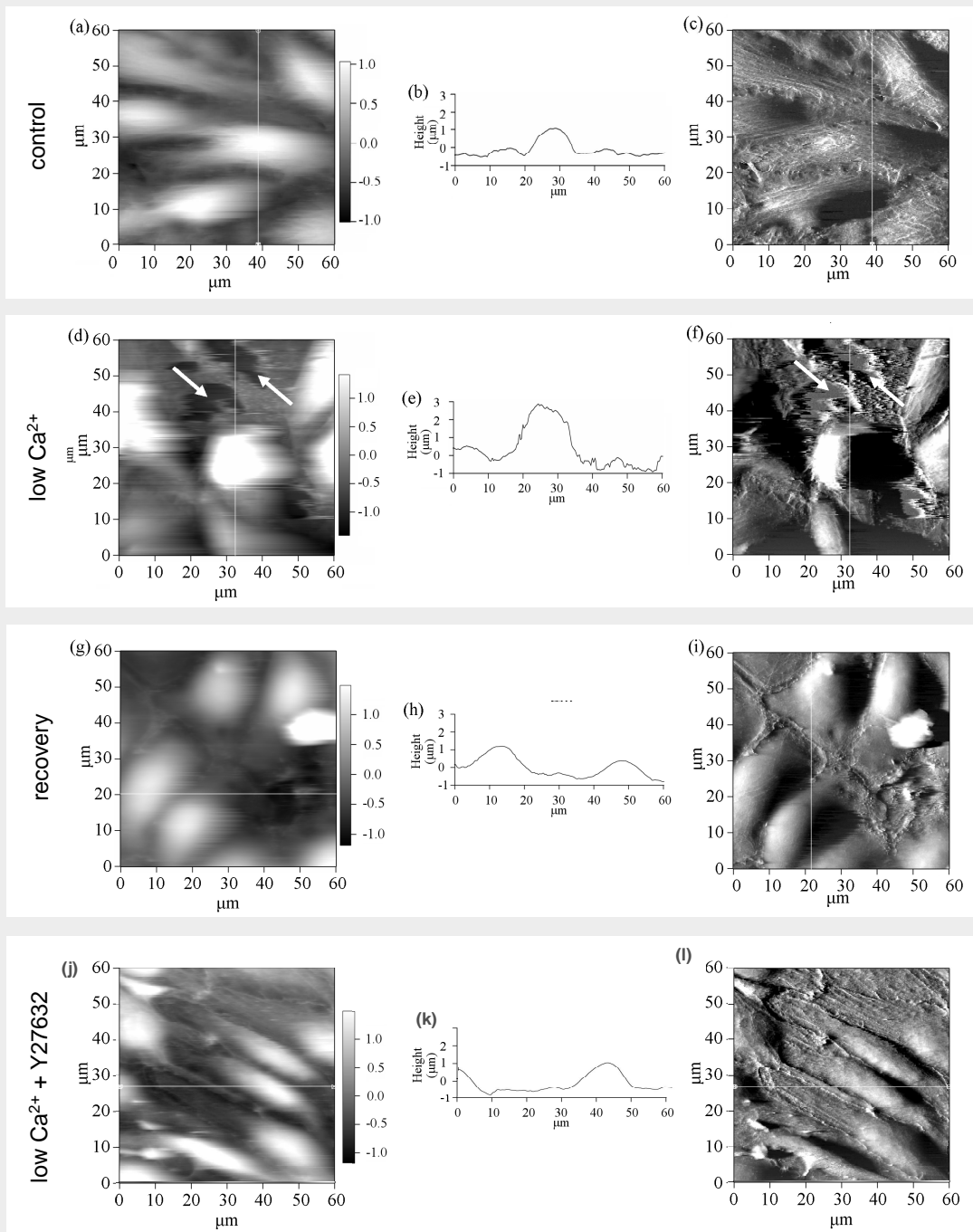


Fig. 5. Effect of depletion and readdition of extracellular Ca^{2+} on rat brain endothelial cells.

Cultures grown to confluency in normal Ca^{2+} containing medium (control: a, b, c), were exposed to a 150 min long depletion of extracellular Ca^{2+} (low Ca^{2+} : d, e, f), followed by readdition of the original medium (recovery: g, h, i) or kept in Ca^{2+} -free medium containing 10 μM Y27632 for 150 min (low Ca^{2+} + Y27632: j, k, l). 60x60 μm^2 AFM height image (a, d, g, j), height profile along the line seen on the image (b, e, h, k) and deflection image (c, f, i, l) are shown. Arrows indicate the surface of the culture dish.

3.1.2. Rho-kinase plays an important role in the Ca²⁺ depletion-induced disassembly of endothelial tight and adherens junctions

Changes in the localization of junctional proteins after Ca²⁺ depletion and readdition were studied by immunofluorescence labeling. As expected, Ca²⁺ depleted monolayers showed a partial disappearance of ZO-1 (Fig. 6 b), claudin-5 (Fig. 6 h) and β -catenin (not shown) from the cell membrane. The process was reversible: during the recovery phase the cells regained the continuous membrane staining of the junctional proteins (Fig. 6 c and i).

Ca²⁺ depletion-induced disassembly of the junctional complex could be partially inhibited by the Rho-kinase inhibitor Y27632 (Fig. 6 e and k). The inhibitor did not have major effects on the control cells and on the recovery phase (Fig. 6 d, j and f, l, respectively).

3.1.3. Cytoskeletal changes after Ca²⁺ depletion are Rho-kinase dependent

Since junctional proteins are directly linked to the actin cytoskeleton and Rho-kinase is known to be implicated in actin reorganization, we performed fluorescence staining of the actin cytoskeleton using phalloidin (Fig. 7 a-d). In control cells we observed the presence of cytoplasmic stress fibers and some peripheral actin filaments at the level of the intercellular junctions (Fig. 7 a). In low Ca²⁺ medium an obvious cell-cell dissociation was observed and an actin ring was formed partially co-localizing with the disintegrated junctions (Fig. 7 c). The Rho-kinase inhibitor Y27632 prevented the Ca²⁺ depletion-induced changes in the actin organization (Fig. 7 d).

We monitored the changes of submembranous cytoskeletal fibers and cell-cell contacts using AFM as well. The actin ring formed after extracellular Ca²⁺ depletion could also be observed on AFM images (Fig. 7 e-g) and was not identical with the marginal folds described by Schrot *et al.* (2005).

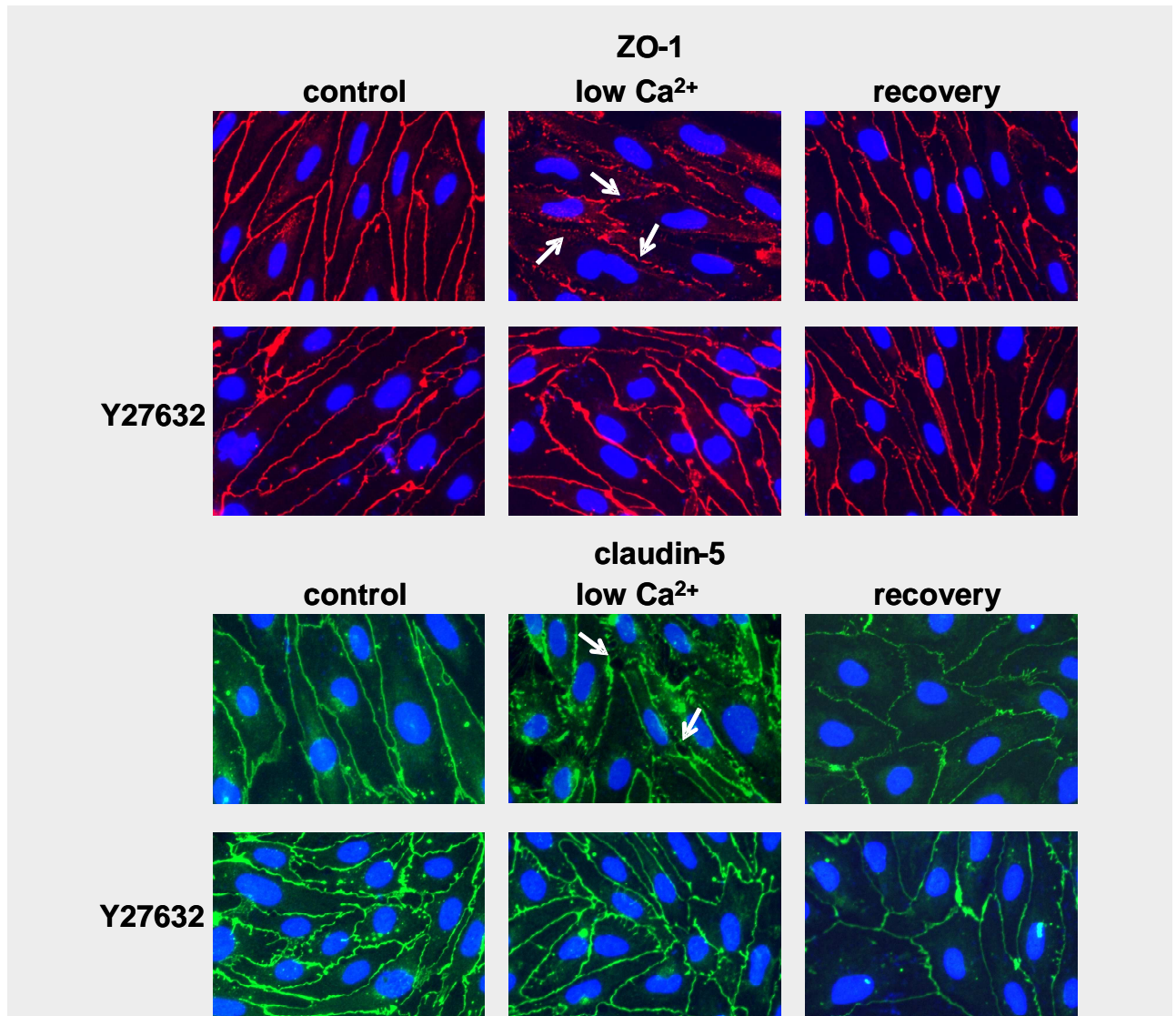


Fig. 6. Effect of Rho-kinase inhibitor Y27632 on the localization of junctional proteins in Ca^{2+} -switch.

Primary rat brain endothelial cells were cultured until confluency (a, d, g, j) and exposed to Ca^{2+} depletion for 150 min (b, e, h, k), followed by 4 h repletion (c, f, i, l) in the presence or absence of 10 μM Y27632. The cells were fixed in different phases of the experiment and stained for tight junction proteins (ZO-1 or claudin-5). One representative of three independent experiments is shown. Arrows indicate the disruption of the junctional staining. Bars = 20 μm .

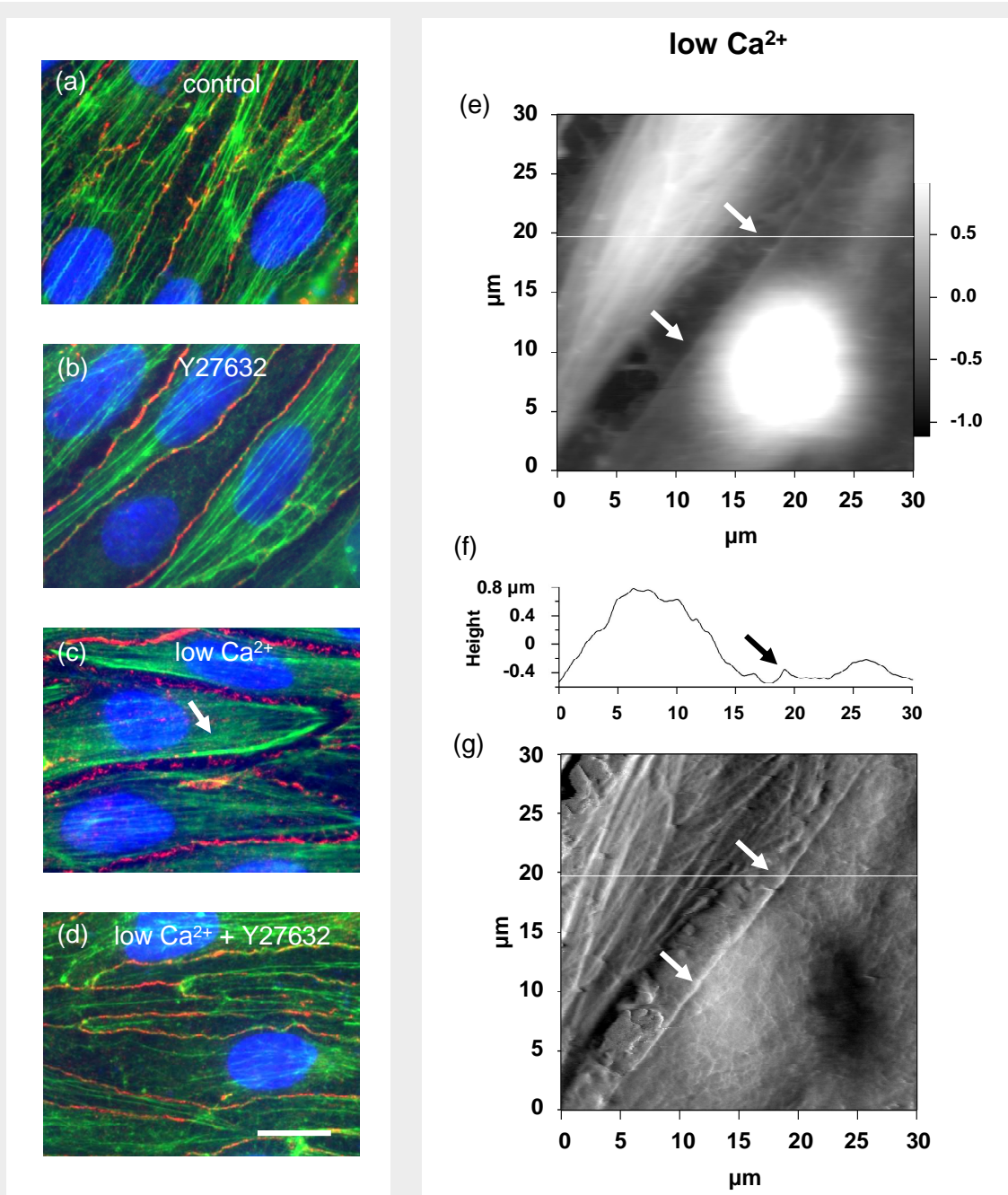


Fig. 7. Effect of Rho-kinase on the actin cytoskeleton of primary rat brain endothelial cells exposed to Ca^{2+} -switch.

Cells were cultured until confluency (a), then exposed to 10 μM Y27632 (b) or Ca^{2+} depletion for 150 min in the presence or absence of 10 μM Y27632 (c, d). The cells were fixed and stained with Alexa488-labelled phalloidin (green), anti-ZO-1 antibody (red) and Hoechst 33258 (nuclei, blue). Bar = 10 μm . (e, f, g): $30 \times 30 \mu\text{m}^2$ AFM height image (e), height profile (f) and deflection image (g) of Ca^{2+} depleted cerebral endothelial cells. Arrows indicate the actin ring formed in low Ca^{2+} medium.

3.2. Effects of hyperosmotic stress

3.2.1. Hyperosmotic stress induces activation of the Axl-Akt pathway

In our previous studies we have shown that hyperosmotic mannitol induces a strong phosphorylation on tyrosine residues in CECs (Farkas *et al.*, 2005). To further identify target proteins of tyrosine phosphorylation an antibody array screening was applied using a matrix loaded with antibodies directed mainly against signaling molecules.

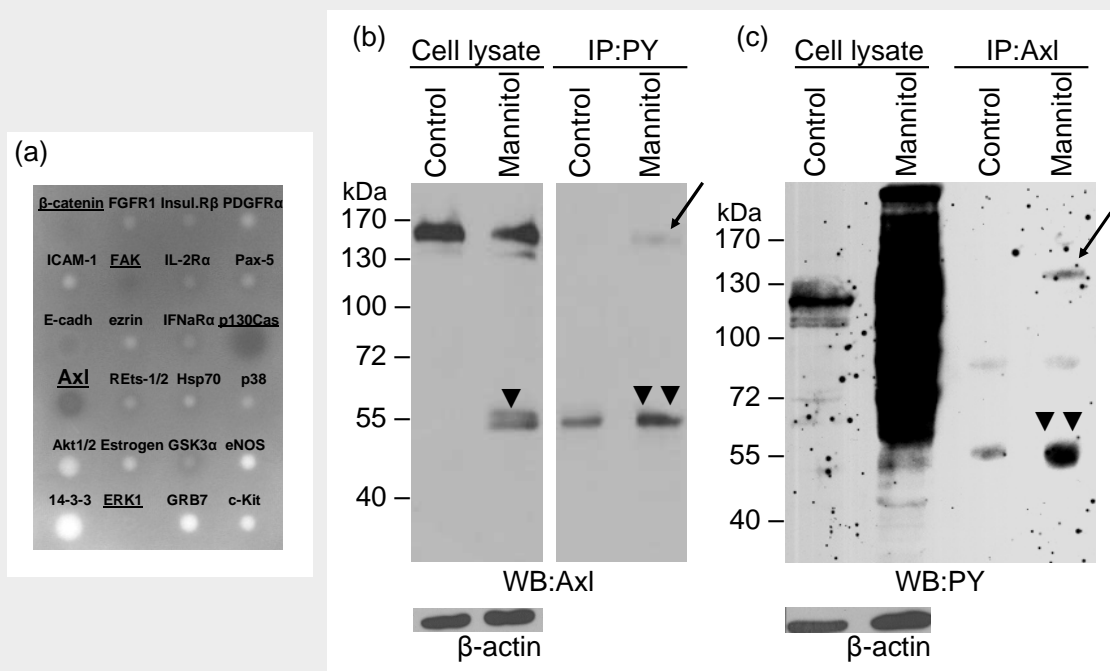


Fig. 8. Tyrosine phosphorylation of Axl induced by mannitol.

(a): Detection of tyrosine phosphorylated proteins using antibody array. CECs were treated with 20% mannitol for 30 min. The antibody array was incubated with the cell homogenate and stained with anti-phosphotyrosine antibody. Identity of the proteins of interest was determined from the position on the membrane. (b, c): Detection of phospho-Axl using immunoprecipitation. CECs were treated with 20% mannitol for 30 min. Immunoprecipitation (IP) was performed using anti-phosphotyrosine (PY) antibody and blots were stained with anti-Axl antibody (b) or the samples were immunoprecipitated using anti-Axl antibody and Western-blot was performed with anti-phosphotyrosine antibody (c). Representative blots of three independent experiments are shown. Arrows indicate the phosphorylated 140 kDa Axl protein. Arrowheads indicate cleavage products. β -actin was used as loading control.

Using this method we found β -catenin, the MAP kinase ERK1, p130Cas, focal adhesion kinase (FAK) and the receptor tyrosine kinase Axl to become phosphorylated (Fig. 8 a). In our previous studies we have already shown that β -catenin and ERK are targets of mannitol-induced

phosphorylation in CECs (Farkas *et al.*, 2005). Literature data are available confirming the phosphorylation of p130Cas and FAK in response to hyperosmosis (Ueno *et al.*, 2001; Lunn *et al.*, 2004).

To prove that Axl can indeed be phosphorylated under hypertonic conditions we performed immunoprecipitation studies using anti-phosphotyrosine antibody (Fig. 8 b) and anti-Axl antibody as well (Fig. 8 c). Both approaches confirmed the tyrosine phosphorylation of Axl after treatment of the cells with 20% mannitol for 30 min.

To test the activation of the possible downstream elements of Axl signaling we investigated the phosphorylation of Akt (protein kinase B). RNA interference was used to specifically knock down Axl and the result of silencing was controlled using Western-blot with anti-Axl antibody (Fig. 9 a). An almost complete silencing of the Axl protein could be achieved. We found that mannitol was able to induce the phosphorylation (on serine473 residue) and thus the activation of Akt (Fig. 9 b). This phenomenon was prevented by Axl silencing, showing that mannitol-induced Akt activation occurs through the receptor tyrosine kinase Axl.

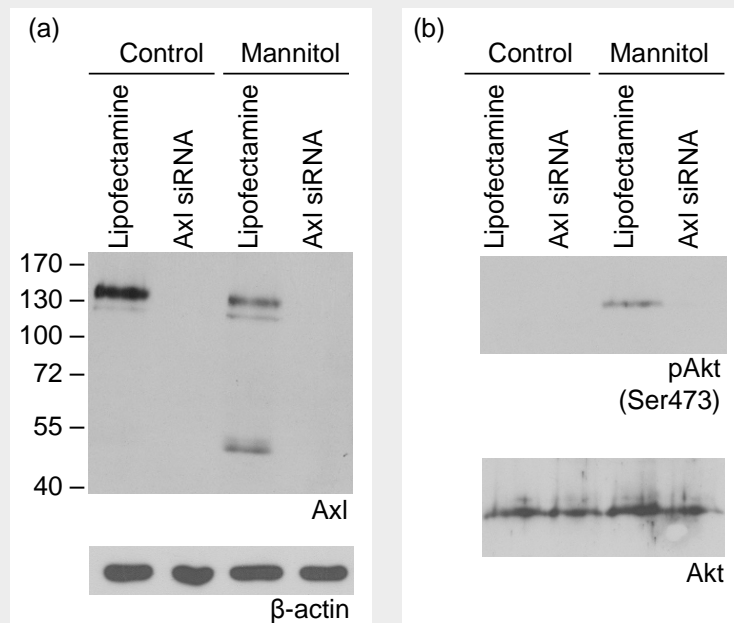


Fig. 9. Activation of Akt in response to hyperosmotic mannitol in cerebral endothelial cells.

Cells were transfected with Axl siRNA construct or Lipofectamine alone and treated with 20% mannitol for 30 min. (a): Axl and its degradation products disappear after silencing. (b): Activation of Axl in response to hyperosmotic mannitol induces phosphorylation of Akt. Blots were stained with anti-phospho-Akt (upper blot) or anti-Akt (lower blot) antibodies. Representative blots of two independent experiments are shown.

3.2.2. Hyperosmosis induces degradation of Axl

We have observed that besides phosphorylation, treatment of CECs with 20% mannitol induced the appearance of a double proteolytic band with an apparent molecular weight of 50-55 kDa (Fig. 10 a), accompanied by a decrease in the intensity of the full size Axl band (Fig. 10 a). Since the antibody recognizes the C-terminal part of the protein, we conclude that this degradation band corresponds to the intracellular domain of Axl. Degradation of Axl proved to be time- and concentration-dependent and was clearly detectable after 10 min of mannitol treatment (Fig. 10 b).

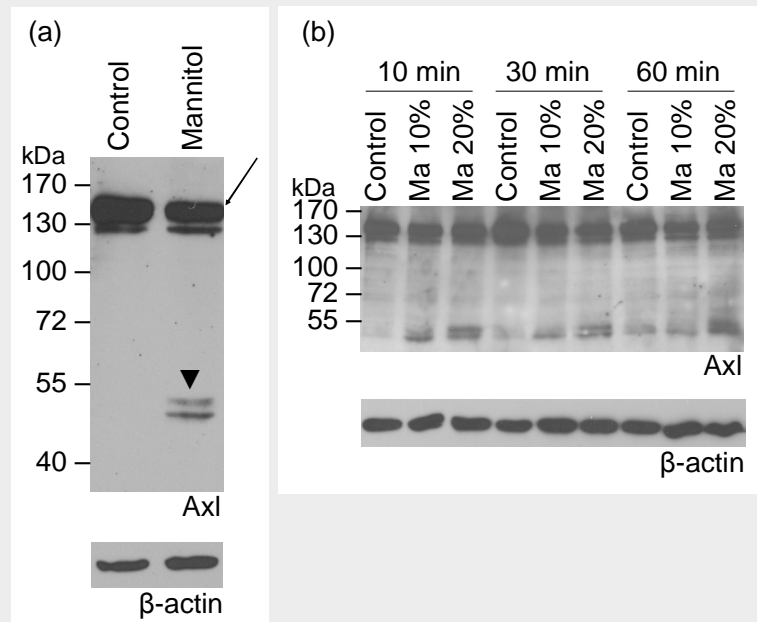


Fig. 10. Effect of mannitol on the cleavage of Axl.

CECs were treated with 20% mannitol for 30 min and blots were stained with anti-Axl antibody. Arrows indicate the location of the whole Axl protein, arrowheads show the degradation products of Axl (a). One representative of ten independent experiments is presented. (b): Time- and concentration-dependence of Axl degradation. CECs were treated with 10 or 20% mannitol for 10, 30 or 60 min and blots were stained with anti-Axl antibody.

No changes in the expression of either Axl or its ligand Gas6 were observed at mRNA level (Fig. 11).

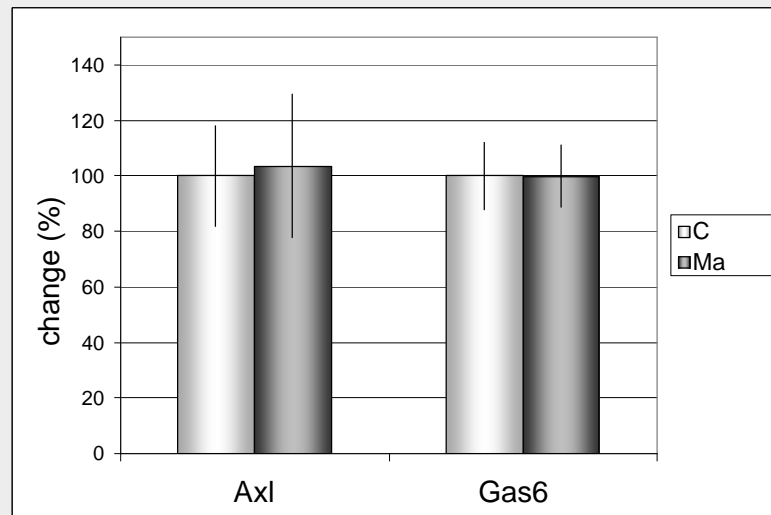


Fig. 11. Expression of Axl and Gas6 mRNA in CECs.

Real-time PCR was performed to assess the expression of Axl and Gas6 in response to mannitol. The housekeeping gene GAPDH was used as internal control. Data represent percentage values compared to control (mean \pm SEM) calculated from four independent experiments. C = control, Ma = mannitol.

We investigated the changes in the localization of Axl in response to mannitol treatment. Under control conditions Axl staining was diffuse, whereas treatment of CECs with 20% mannitol led to the appearance of a conspicuous perinuclear staining (Fig. 12).

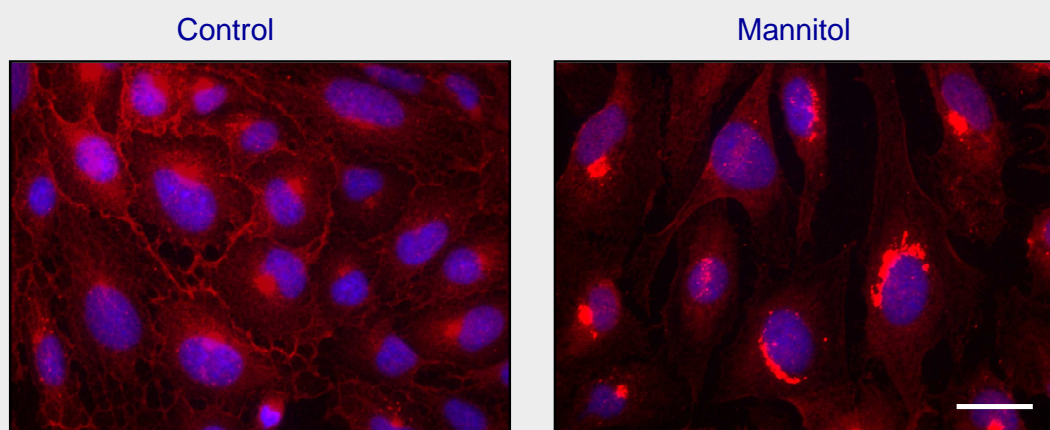


Fig. 12. Immunofluorescence staining of Axl in CECs.

CECs were cultured on glass coverslips, treated with 20% mannitol for 30 min, fixed and stained with anti-Axl antibody (red) and Hoechst 33258 (nuclei, blue). One representative image of three independent experiments is shown. Scale bar = 20 μ m.

We have tested the effect of other osmotic agents (arabinose, sodium chloride and urea) in similar osmotic concentrations to 1.1 M mannitol (additional 1100 mOsmol/l). When osmotic stress was caused by poorly cell permeable agents (mannitol, NaCl or arabinose) we observed the appearance of the cleavage products with a parallel decrease in the main Axl band (Fig. 13 a). However, the cell permeable urea did not induce Axl cleavage (Fig. 13 a), suggesting that cellular shrinkage is probably responsible for Axl degradation. Other stress factors like oxidative stress (DMNQ treatment), Ca^{2+} or glucose deprivation (not shown) or high glucose concentration (8 g/l) did not cause alterations in Axl levels (Fig. 13 b). Degradation of Axl in response to hypertonic stress could be detected not only in CECs but in other cell types like Madin-Darby Canine Kidney (MDCK) or the rat glioma cell line RG2 as well (Fig. 13 c).

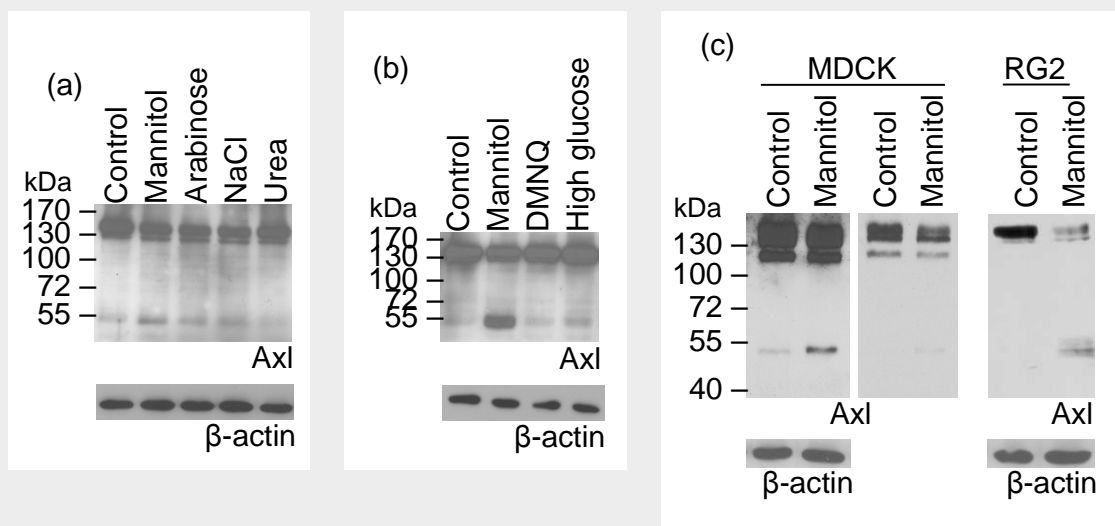


Fig. 13. Specificity of hyperosmotic stress-induced Axl degradation.

(a): Effect of different osmotic agents on the degradation of Axl. Cells were treated with 1.1 M mannitol, arabinose, urea or 0.55 M NaCl, respectively for 30 min. (b): Effect of different stress factors on the degradation of Axl. Cells were treated with: 20% mannitol, 10 μM DMNQ or 8 g/l glucose, respectively. (c): Degradation of Axl in MDCK and RG2 cells in response to mannitol treatment. The first two panels show the same blot with different exposure times to visualize changes in Axl and its degradation products. β -actin was used as loading control.

To identify the mechanisms by which Axl degradation is regulated we have used a series of inhibitors of different signaling pathways and protease inhibitors. Inhibition of nuclear factor-kappa B (NF- κB , using PDTC), Rho-kinase (using Y27632), Ca^{2+} channel (using verapamil) (Fig. 14 a), protein kinase C (PKC, using bisindolylmaleimide), phosphatidylinositol 3-kinase (PI3K, using wortmannin), ERK 1/2 (using U0126) or Src kinase (using PP1) (Fig. 14 b) did not

affect the degradation of Axl. Caspase inhibition (using zVAD), inhibition of calpain (using calpeptin) (Fig. 14 b), and the use of cysteine, serine or aspartic protease inhibitors (E64, leupeptin, pepstatin) (Fig. 14 c) were also ineffective in reducing the degradation of Axl.

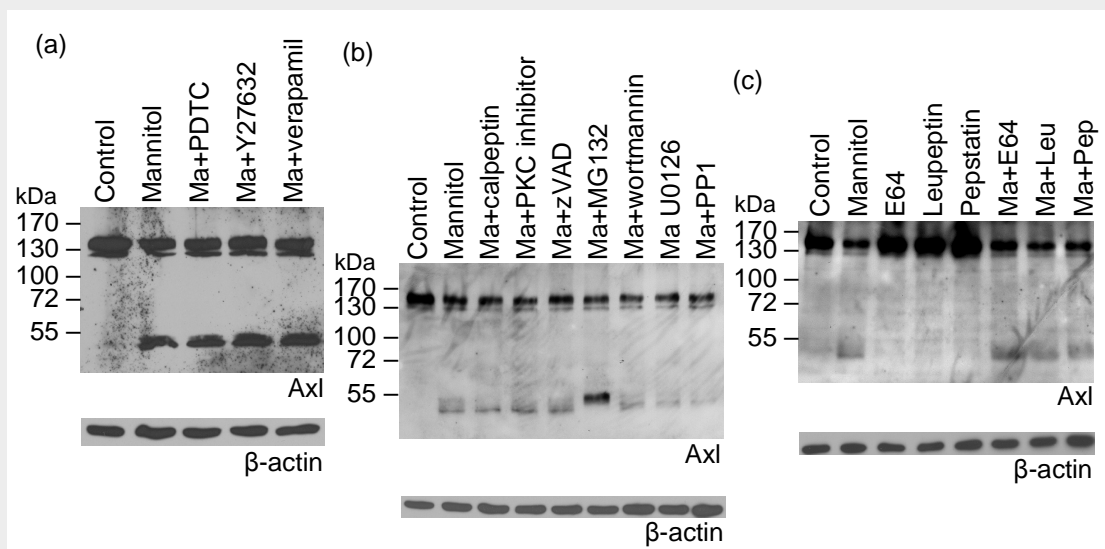


Fig. 14. Mechanism of Axl degradation.

Cells were treated with 20% mannitol for 30 min in the presence or absence of different inhibitors: NF κ B inhibitor (10 μ M PDTC), Rho-kinase inhibitor (10 μ M Y27632), L-type Ca²⁺ channel blocker (10 μ M verapamil) (a), calpain inhibitor (10 μ M calpeptin), PKC inhibitor (1 μ M bisindolylmaleimide), caspase inhibitor (25 μ M zVAD), proteasome inhibitor (50 μ M MG132), PI3kinase inhibitor (1 μ M wortmannin), ERK 1/2 inhibitor (10 μ M U0126) and Src inhibitor (10 μ M PP1) (b) or protease inhibitors (100 μ M E64, 50 μ M leupeptin, 10 μ M pepstatin) (c). β -actin was used as loading control.

On the other hand, the matrix metalloproteinase inhibitor GM6001 was able to almost completely inhibit the degradation of Axl induced by hyperosmotic mannitol (Fig. 15 a, b).

We investigated the solubility of the different Axl bands. Only the lower band of the degradation products proved to be soluble in detergent-free buffer. Both the whole protein and the upper degradation band were water-insoluble and detergent (i.e. Triton X-100) soluble (Fig. 15 c). The proteasome inhibitor MG132 induced the disappearance of the lower (water-soluble) degradation fragment parallelly with the intensification of the upper (detergent-soluble) cleavage product, however, no change in the amount of the 140 kDa band was seen (Fig. 15 c).

These results suggest that cleavage of Axl occurs in two steps: the metalloproteinase-dependent cleavage is followed by proteasomal degradation.

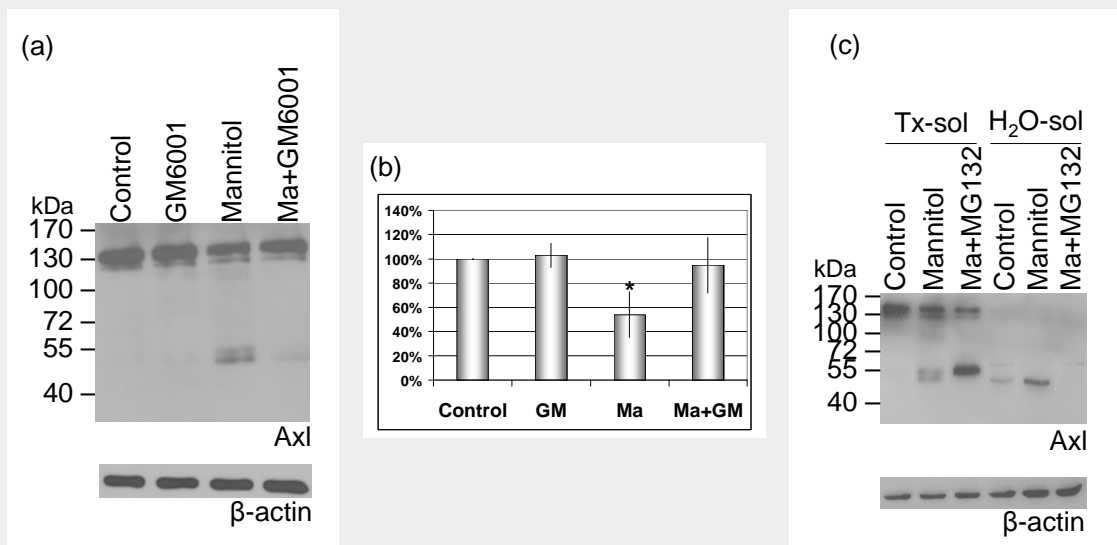


Fig. 15. Role of metalloproteinases and the proteasome in Axl degradation.

(a): The metalloprotease inhibitor GM6001 was able to inhibit Axl degradation. One representative of five independent experiments is shown. (b): Densitometric analysis of Axl Western-blot. Data represent percentage values of the 140 kDa Axl band intensity compared to control (mean \pm SD) calculated from five independent experiments. *: $p < 0.001$ compared to control using t-test. (c): Role of the proteasome. Protein samples were prepared from CECs treated with 20% mannitol and 50 μ M MG132 either in Triton X-100 containing buffer or detergent-free buffer. One representative of three independent experiments is presented. β -actin was used as loading control.

3.2.3. Phosphorylation and degradation of Axl are not directly related

To study the possible relationship between the phosphorylation and degradation of Axl we investigated the time course of Axl phosphorylation and degradation. Axl becomes phosphorylated after 2 min and reaches its maximum at 15 min whereas the degradation starts between 5-15 min (Fig. 16 a). Pervanadate, a strong phosphatase inhibitor induced the phosphorylation of Axl but did not cause its degradation indicating that the cleavage of Axl is not induced by tyrosine phosphorylation (Fig. 16 b). This was also supported by the fact that the tyrosine kinase inhibitor genistein, which inhibited the phosphorylation of Axl, did not inhibit its degradation (Fig. 16 b). Furthermore, the metalloproteinase inhibitor GM6001 which inhibited the degradation of Axl did not affect activation of Akt, a downstream element of Axl signaling (Fig. 16 c).

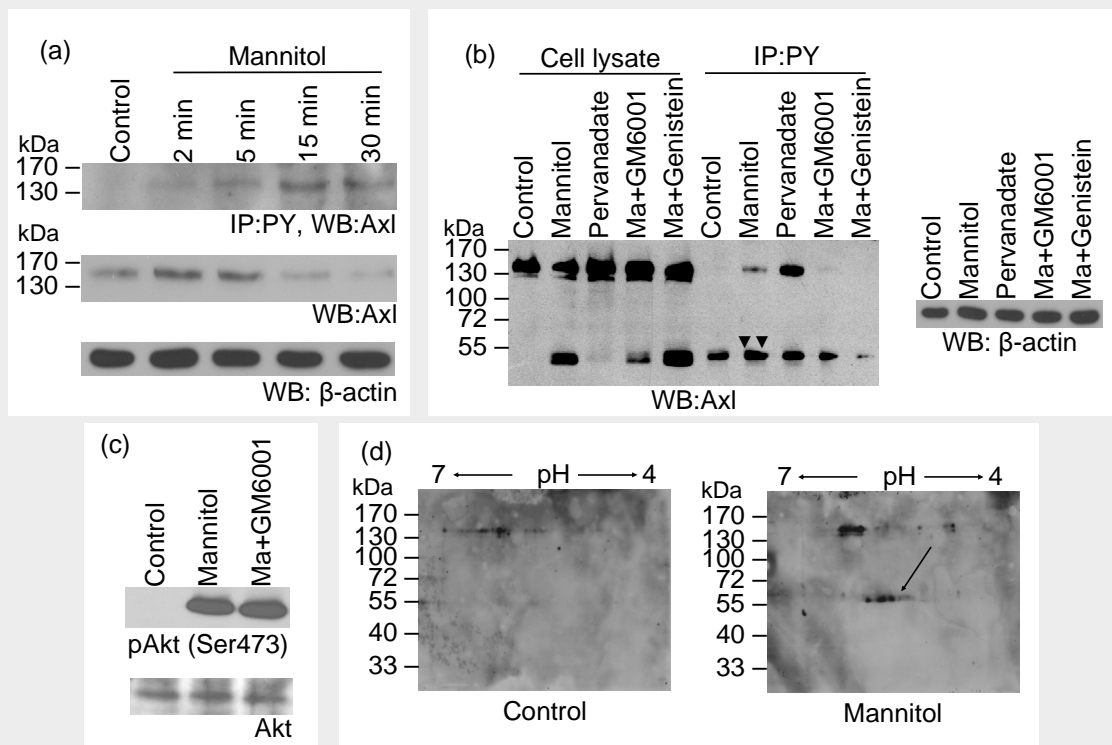


Fig. 16. Relationship between degradation and phosphorylation of Axl.

(a): Time course of Axl phosphorylation (a, upper blot) and Axl degradation (a, lower blot). Cells were treated with 20% mannitol for the indicated times. Immunoprecipitation was performed using anti-phosphotyrosine antibody. Axl Western-blot was performed from the immunoprecipitated samples (a, upper blot) and the cell lysates (a, lower blot). (b): Phosphorylation of the degradation products. Cells were treated for 30 min with 20% mannitol, 50 μ M pervanadate, 20% mannitol and 10 μ M GM6001 or 20% mannitol and 100 μ M genistein, respectively. Immunoprecipitation was performed using anti-phosphotyrosine antibody, followed by Axl Western-blot. Double arrowheads indicate the phosphorylated cleavage products of mannitol-treated samples. β -actin was used as loading control. (c): GM6001 does not influence phosphorylation of Akt. Cells were treated with 20% mannitol for 30 min in the presence or absence of 10 μ M GM6001 and blots were stained with anti-phospho-Akt (upper blot) or Akt (lower blot) antibodies. (d): Investigation of Axl using two-dimensional electrophoresis combined with Western-blot. Cells were treated for 30 min with 20% mannitol. Proteins of cell lysates were separated in two dimensions based on their isoelectric point and molecular weight, followed by Western-blot analysis using anti-Axl antibody.

Our results obtained from phosphotyrosine immunoprecipitation studies suggest that the degradation products of Axl are phosphorylated in mannitol treated cells (Fig. 16 b, Fig. 8 b, c). The tyrosine kinase inhibitor genistein reduced the mannitol-induced phosphorylation of the Axl degradation products to control levels (Fig. 16 b). Presence of multiple spots at the level of the 55 kDa degradation products on Axl Western-blot performed on two-dimensional gels may also indicate differently phosphorylated forms of the protein (Fig. 16 c).

3.2.4. Axl is involved in the regulation (inhibition) of hyperosmotic mannitol-induced apoptosis

To gain insight into the role of mannitol-induced Axl activation we have counted the number of apoptotic cells after mannitol treatment in control and Axl-silenced cells. The knockdown was almost complete in Axl siRNA-transfected cells and the scrambled sequence did not affect Axl expression (Fig. 17 a). The rate of apoptosis was determined based on cleaved caspase-3 staining. 30 min mannitol treatment did not induce significant changes in the number of apoptotic cells. However, after 3 h mannitol treatment a more than 100% increase was detectable: from $2.83 \pm 0.10\%$ in Lipofectamine treated and $2.55 \pm 0.21\%$ in scrambled RNA-transfected cells to $5.83 \pm 0.21\%$ and $5.50 \pm 0.85\%$, respectively (Fig. 17 b). Axl silencing induced a more than 50% increase in the number of apoptotic cells in control conditions, and a more than 40% increase in mannitol treated cells (Fig. 17 b). Similar results were obtained when apoptosis was assessed based on nuclear morphology (not shown).

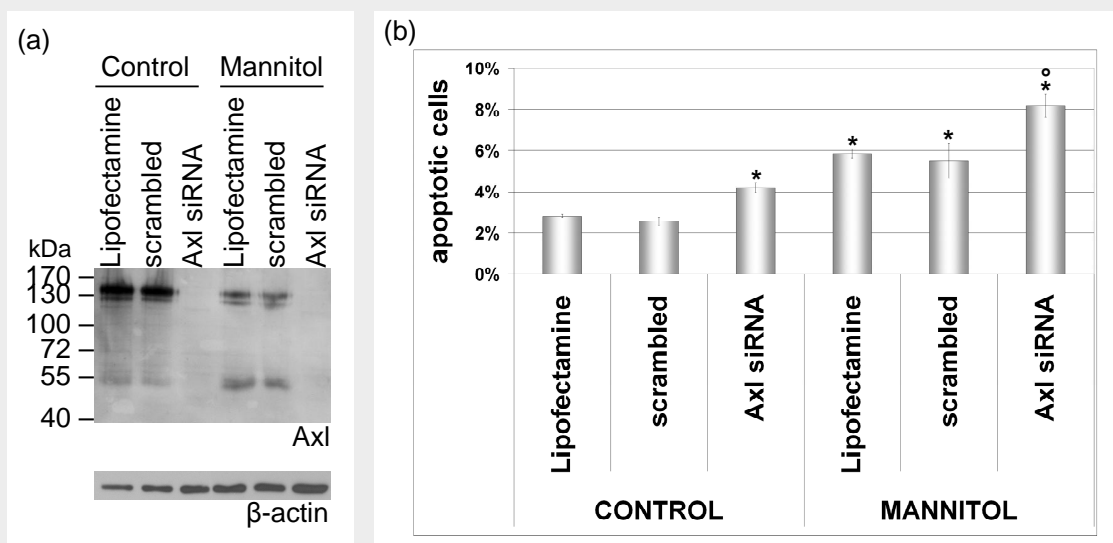


Fig. 17. Role of Axl in mannitol-induced apoptosis.

(a): Silencing of Axl. (b): Investigation of apoptosis after Axl silencing and mannitol treatment. Cells were cultured on glass coverslips and were transfected with Axl siRNA, scrambled RNA construct or treated with Lipofectamine alone, followed by treatment with 20% mannitol for 3 h. The rate of apoptosis was determined based on cleaved caspase-3 immunostaining. Values represent the mean \pm SD calculated from two independent experiments. *: $p < 0.05$ compared to Lipofectamine-treated control cells, °: $p < 0.05$ compared to Lipofectamine- and mannitol-treated cells, using ANOVA and LSD post hoc test.

4. DISCUSSION

4.1. Mechanisms regulating changes induced by Ca^{2+} depletion and readdition

The unique barrier properties of brain endothelial cells are partly connected to the junctional complex that seals the intercellular way of transport. Ca^{2+} -dependence of tight and adherens junctions is well documented in kidney and intestinal epithelial cells (Gonzalez-Mariscal *et al.*, 1990; Pitelka *et al.*, 1983; Rothen-Rutishauser *et al.*, 2002; Ivanov *et al.*, 2004(a)), however, much less is known about cerebral endothelial cells. In line with these experimental data obtained in epithelial cells, we observed a disappearance of ZO-1, claudin-5 and β -catenin from the junctions of brain endothelial cells in response to Ca^{2+} depletion.

However, the mechanisms of junctional dissociation are still incompletely understood. In T84 epithelial cells it has been shown that in response to Ca^{2+} depletion a clathrin mediated endocytosis of junctional proteins occurs (Ivanov *et al.*, 2004(b)). During the recovery phase these proteins are probably redirected from the intracellular storage compartments to the intercellular junctional region. This has been shown in MDCK cells: chloroquine, a drug which prevents exocytosis, blocked sealing of tight junctions (Gonzalez-Mariscal *et al.*, 1990). In endothelial cells a similar mechanism is presumed to play role, however, we have no direct data supporting this hypothesis.

The junctions are connected in a complex way to the actin cytoskeleton which plays a significant role in the regulation of paracellular permeability. Cytoskeletal changes might also contribute to alterations in the junctional integrity. In intestinal epithelial cells it has been shown that removal of extracellular Ca^{2+} caused the activation of myosin light chain kinase and the centripetal retraction of perijunctional actin and myosin filaments (Ma *et al.*, 2000). Another study has shown that reorganization of the apical actin cytoskeleton involves cofilin-1-dependent depolymerization and Arp2/3-assisted repolymerization of actin filaments, as well as myosin IIA-mediated contraction (Ivanov *et al.*, 2004(a)). Ca^{2+} depletion-induced reorganization of the actin

cytoskeleton resulted in contractile rings colocalizing with internalized junctional proteins (Ivanov *et al.*, 2004(a)).

We have studied the cytoskeletal alterations induced by Ca^{2+} depletion and readdition in CECs using atomic force microscopy. This high resolution technique makes possible to follow changes at cellular and subcellular level in living cells. We have shown that depletion of extracellular Ca^{2+} induces characteristic morphological changes in cerebral endothelial cells: appearance of intercellular gaps in a previously confluent monolayer and increase in the height of the cells. This was accompanied by changes in the actin-cytoskeleton, as revealed by both atomic force microscopy and phalloidin staining: formation of a peripheral actin ring partially colocalizing with the disintegrated junctions.

Moreover, we have shown that Ca^{2+} depletion-induced morphological, cytoskeletal and junctional changes were dependent on Rho-kinase. The small G protein RhoA and its downstream effector Rho-kinase are both expressed in endothelial cells and are involved in the regulation of several cellular processes. They are key regulators of actin reorganization, cell motility, adhesion and permeability (Hopkins *et al.*, 2007). The role of Rho-kinase in the regulation of junctional disassembly has been recently suggested in epithelial cells. Fan *et al.*, (2007) describe a mechanism of cell contact regulated epithelial to myofibroblast transition via a Rho/Rho-kinase dependent pathway. It has also been demonstrated that the activity of the Rho/Rho-kinase/myosin pathway antagonizes the early steps of tight junction assembly in cells lacking the polarity protein Par-3 (Chen and Macara, 2006).

Further studies are needed to elucidate the exact role of Rho-kinase in the disassembly of the junctions in CECs. It is possible that Rho-generated cytoskeletal tension leads to the disruption of the junctions and cell-cell contacts, however, a direct phosphorylation of the junctional proteins cannot be excluded.

Morphological, cytoskeletal and junctional changes induced by Ca^{2+} depletion proved to be reversible: shortly after readdition of the physiological Ca^{2+} concentration the intercellular gaps gradually disappeared, the cells regained their original height and shape, and the continuous membrane staining of the junctional proteins was restored. The cytoskeleton is likely to play an important role in the recovery too. However, this process is probably Rho-kinase independent,

because addition of the Rho-kinase inhibitor Y27632 did not result in any delay in the junctional reassembly.

In conclusion, our data suggest that Rho-kinase may play an important role in the regulation of the actin-cytoskeleton and in the disassembly of tight junctions in the Ca^{2+} -switch model. These mechanisms are likely responsible for the reorganization of the junctions under physiological and/or pathological conditions.

4.2. Hyperosmotic stress-induced Axl activation and cleavage

Disruption of the BBB by rapid intracarotid infusion of a hyperosmolar solution has been used both experimentally and clinically to increase the transport of different substances to the CNS. We have investigated the mechanisms of hyperosmotic stress-induced changes at cellular and molecular levels. In our previous studies we have shown that osmotic stress induces marked changes in cerebral endothelial cells, including morphological, volume and elasticity changes measured by AFM (Bálint *et al.*, 2007). Moreover, we have shown that mannitol in hyperosmotic concentration induces a strong phosphorylation on tyrosine residues in a broad spectrum of proteins ranging between 50-200 kDa (Farkas *et al.*, 2005). Among targets of tyrosine phosphorylation were β -catenin and the non-receptor tyrosine kinase Src (Farkas *et al.*, 2005). In order to identify other targets of tyrosine phosphorylation, we have applied a screening approach based on an antibody array. We could identify three additional proteins to become tyrosine phosphorylated in response to hyperosmotic stress: p130Cas (p130 Crk-associated substrate), FAK (focal adhesion kinase) and Axl. Moreover, we could confirm our earlier finding that β -catenin and ERK1 are tyrosine phosphorylated in CECs in response to hyperosmotic mannitol treatment.

p130Cas is an Src substrate signaling molecule localized to focal adhesions (Harte *et al.*, 1996) and is involved in several processes including motility, adhesion, proliferation and survival (for review see: Defilippi *et al.*, 2006). p130Cas has already been shown to become tyrosine phosphorylated in adipocytes in response to osmotic stress (Ueno *et al.*, 2001). FAK which is in close interaction with p130Cas (Polte *et al.*, 1995) has also been shown to be tyrosine phosphorylated under hyperosmotic conditions in fibroblasts and endothelial cells of non-cerebral origin (Lunn *et al.*, 2004; Malek *et al.*, 1998).

By demonstrating that Axl becomes phosphorylated on tyrosine residues and Akt becomes phosphorylated on serine473 residue only in cells expressing Axl, we could identify a new signaling pathway activated by osmotic stress in CECs.

Furthermore we have shown that Axl is cleaved in response to hyperosmosis, the C-terminal products having an apparent molecular weight of about 50-55 kDa. Axl has been shown to be posttranslationally regulated by proteolysis (O'Bryan *et al.*, 1995) resulting in the generation of soluble Axl (Costa *et al.*, 1996). Our results show that the mannitol-induced cleavage of Axl is metalloproteinase-dependent which is in line with previous reports demonstrating the role of disintegrin-like metalloproteinase ADAM 10 in the cleavage of Axl (Budagian *et al.*, 2005). The role of Axl cleavage and the function of soluble Axl are still far from being completely understood. Soluble Axl has been detected in mouse serum and is constitutively released by murine primary and transformed cells (Budagian *et al.*, 2005). It may play role in the regulation of the bioavailability of the Axl ligand Gas6 by binding and thus inactivating it. Activation of PKC has also been shown to trigger cleavage of Axl and the proteolytic cleavage site was found to localize to a 14-amino acid region (VKPSTPAFSWPWW) between the second fibronectin and the transmembrane domain (O'Bryan *et al.*, 1995). However, in CECs the PKC inhibitor bisindolylmaleimide was able to inhibit only PMA (phorbol myristyl acetate)-, but not hyperosmosis-induced Axl degradation (data not shown) suggesting that there is a difference between hyperosmosis- and PKC-induced Axl degradation.

It is well known that Axl is expressed at high levels in gliomas, mediating both tumor growth and angiogenesis (Vajkoczy *et al.*, 2006). Specific targeting of Axl may become a promising target of therapy of these tumors. Our results have shown that hyperosmotic mannitol-induced cleavage of Axl was not restricted to cerebral endothelial, or tight junction-expressing (endothelial and epithelial) cells, but glioma cells as well. Interestingly, when NaCl or arabinose were used instead of mannitol in the same osmotic concentration, Axl cleavage occurred in the same way, however, the cell permeable urea did not induce Axl degradation. Therefore, we assume that cellular shrinkage might be responsible for this phenomenon.

We found that induction of tyrosine phosphorylation of Axl did not lead to its degradation, and inhibition of tyrosine phosphorylation did not influence the mannitol-induced cleavage of

Axl. These findings suggest that there is no direct relationship between phosphorylation and cleavage of Axl. Using an antibody recognizing the C-terminal region of Axl we have observed that the degradation products containing the catalytically active intracellular domain of Axl remain phosphorylated. Mainly the upper (Triton X-100 soluble) degradation band proved to be phosphorylated, however, the two degradation bands seem to be different cleavage products and not differently phosphorylated forms of the same cleavage products. This is supported by the fact that treatment with genistein which inhibited the phosphorylation of Axl, did not inhibit the appearance of two cleavage products (Fig. 16 b). Moreover, the appearance of the lower degradation band was prevented by the proteasome inhibitor MG132 (Fig. 15 c) supporting that in hyperosmotic mannitol-treated cells the metalloproteinase-mediated cleavage was followed by a proteasomal cleavage, resulting in a water-soluble degradation product.

In order to address the functional implications of Axl activation, we have performed knockdown experiments and examined hyperosmotic mannitol-induced apoptosis. It is well documented that hypertonicity induces apoptosis in different cell types (for review see: Bortner and Cidlowski, 2007). On the other hand, activation of the Axl-Akt pathway is involved in cell survival and anti-apoptotic mechanisms (for review see: Hafizi and Dahlbäck, 2006(b)). We have found an approximately 90-100% increase in apoptosis after treatment with hyperosmotic mannitol. The relatively low absolute levels of apoptosis are apparently in contrast with previous observations by Malek *et al.* (1998), who have shown that treatment of bovine aortic endothelial cells with 600 mOsmol/l mannitol for 3 h induced an increase in the rate of apoptosis from 1.2% to 42%. However, microvascular endothelial cells may react differently to apoptotic stimuli than macrovascular endothelial cells. It has been shown that hyperglycaemic conditions significantly increased apoptosis in macrovascular endothelial cells, while increasing viability and inhibiting apoptosis in microvascular endothelial cells (Duffy *et al.*, 2006). In a previous study it has been shown that prolonged oxidative stress even under hypoglycaemic conditions was able to induce an apoptosis of about 7-20% with great interspecies variability (Bresgen *et al.*, 2003). We observed that Axl silencing increased the rate of apoptosis in hyperosmotic mannitol-treated cells, therefore we assume that activation of Axl may be a protective mechanism against mannitol-induced apoptosis.

Further studies are needed to clarify if Axl is involved in the hyperosmotic mannitol-induced BBB opening. A direct relationship between Axl signaling and proteins of the tight junction has not been shown so far. However, it is well known that a large number of signaling pathways are able to regulate junctional functions, and tyrosine phosphorylation may play an important role in this process.

In conclusion, we have identified Axl as an important element of hyperosmosis-induced signaling in cerebral endothelial cells, and we suggest that Axl could play an important role in the adaptive response of cells to hyperosmotic stress.

Understanding the role of different signaling molecules in the regulation of brain endothelial functions is important because they may become potential targets for future therapeutical approaches. To summarize our results, we have studied signaling pathways activated by Ca^{2+} depletion and hyperosmotic stress, respectively in brain endothelial cells. We have shown that:

1. Rho-kinase plays an important role in the Ca^{2+} depletion-induced cytoskeletal reorganization and disintegration of interendothelial contacts;
2. Axl is activated and cleaved in response to hyperosmotic stress in cerebral endothelial cells.

Our data give insight into different stress factor-activated mechanisms in the brain endothelium.

5. SUMMARY

Cerebral endothelial cells, the main components of the blood-brain barrier, are directly exposed to different stress factors. In response to these, they are able to activate a complex network of signaling pathways. In our studies we have addressed the role of two signaling molecules in the brain endothelium, namely Rho-kinase and Axl receptor tyrosine kinase.

Since the presence of a continuous line of tight junctions at intercellular contacts is one of the most important elements of the blood-brain barrier phenotype of cerebral endothelial cells, understanding the regulation of interendothelial junctions is of primordial importance. We have shown that activation of Rho-kinase in response to depletion of extracellular Ca^{2+} is involved in the reorganization of the cytoskeleton, disintegration of tight junctions and formation of intercellular gaps.

We have also studied the role of the receptor tyrosine kinase Axl in cerebral endothelial cells. We have identified the Axl-Akt pathway as a protective mechanism against hyperosmosis-induced apoptosis. However, activation of Axl was followed by its metalloproteinase- and proteasome-dependent degradation. This suggests that osmotic stress leads to the activation of both pro- and anti-apoptotic mechanisms and survival of endothelial cells is precisely regulated.

Taken together, we have identified Rho-kinase and Axl as two important signaling molecules involved in the regulation of different functions of brain endothelial cells. Rho-kinase proved to be involved in the regulation of tight junctions, and therefore affecting one of the specific BBB characteristics of CECs. Axl has been identified as an important element in the regulation of endothelial apoptosis.

6. REFERENCES

1. Abbott NJ, Rönnbäck L, Hansson E. Astrocyte-endothelial interactions at the blood-brain barrier. *Nat Rev Neurosci.* 2006;7:41-53.
2. András IE, Pu H, Tian J, Deli MA, Nath A, Hennig B, Toborek M. Signaling mechanisms of HIV-1 Tat-induced alterations of claudin-5 expression in brain endothelial cells. *J Cereb Blood Flow Metab.* 2005;25:1159-70.
3. Bálint Z, Krizbai IA, Wilhelm I, Farkas AE, Párducz A, Szegletes Z, Váró G. Changes induced by hyperosmotic mannitol in cerebral endothelial cells: an atomic force microscopic study. *Eur Biophys J.* 2007;36:113-20.
4. Binnig G, Quate CF, Gerber C. Atomic force microscope. *Physical Review Letters.* 1986;56:930-933
5. Bortner CD, Cidlowski JA. Cell shrinkage and monovalent cation fluxes: role in apoptosis. *Arch Biochem Biophys.* 2007;462:176-88.
6. Breier G, Breviario F, Caveda L, Berthier R, Schnürch H, Gotsch U, Vestweber D, Risau W, Dejana E. Molecular cloning and expression of murine vascular endothelial-cadherin in early stage development of cardiovascular system. *Blood.* 1996;87:630-41.
7. Bresgen N, Karlhuber G, Krizbai I, Bauer H, Bauer HC, Eckl PM. Oxidative stress in cultured cerebral endothelial cells induces chromosomal aberrations, micronuclei, and apoptosis. *J Neurosci Res.* 2003;72:327-33.
8. Budagian V, Bulanova E, Orinska Z, Duitman E, Brandt K, Ludwig A, Hartmann D, Lemke G, Saftig P, Bulfone-Paus S. Soluble Axl is generated by ADAM10-dependent cleavage and associates with Gas6 in mouse serum. *Mol Cell Biol.* 2005;25:9324-39.
9. Burg MB, Ferraris JD, Dmitrieva NI. Cellular response to hyperosmotic stresses. *Physiol Rev.* 2007;87:1441-74.
10. Chen X, Macara IG. Par-3 mediates the inhibition of LIM kinase 2 to regulate cofilin phosphorylation and tight junction assembly. *J Cell Biol.* 2006;172:671-8.
11. Citi S, Sabanay H, Jakes R, Geiger B, Kendrick-Jones J. Cingulin, a new peripheral component of tight junctions. *Nature.* 1988;333:272-6.
12. Citi S, Sabanay H, Kendrick-Jones J, Geiger B. Cingulin: characterization and localization. *J Cell Sci.* 1989;93:107-22.
13. Costa M, Bellosta P, Basilico C. Cleavage and release of a soluble form of the receptor tyrosine kinase ARK in vitro and in vivo. *J Cell Physiol.* 1996;168:737-44.
14. D'Arcangelo D, Gaetano C, Capogrossi MC. Acidification prevents endothelial cell apoptosis by Axl activation. *Circ Res.* 2002;91:e4-12.

15. D'Arcangelo D, Ambrosino V, Giannuzzo M, Gaetano C, Capogrossi MC. Axl receptor activation mediates laminar shear stress anti-apoptotic effects in human endothelial cells. *Cardiovasc Res.* 2006;71:754-63.
16. de Boer AG, van der Sandt IC, Gaillard PJ. The role of drug transporters at the blood-brain barrier. *Annu Rev Pharmacol Toxicol.* 2003;43:629-56.
17. Defilippi P, Di Stefano P, Cabodi S. p130Cas: a versatile scaffold in signaling networks. *Trends Cell Biol.* 2006;16:257-63.
18. Di Ciano C, Nie Z, Szászi K, Lewis A, Uruno T, Zhan X, Rotstein OD, Mak A, Kapus A. Osmotic stress-induced remodeling of the cortical cytoskeleton. *Am J Physiol Cell Physiol.* 2002;283:C850-65.
19. Di Ciano-Oliveira C, Sirokmány G, Szászi K, Arthur WT, Masszi A, Peterson M, Rotstein OD, Kapus A. Hyperosmotic stress activates Rho: differential involvement in Rho kinase-dependent MLC phosphorylation and NKCC activation. *Am J Physiol Cell Physiol.* 2003;285:C555-66.
20. Duffy A, Liew A, O'Sullivan J, Avalos G, Samali A, O'Brien T. Distinct effects of high-glucose conditions on endothelial cells of macrovascular and microvascular origins. *Endothelium.* 2006;13:9-16.
21. Fan L, Sebe A, Péterfi Z, Masszi A, Thirone AC, Rotstein OD, Nakano H, McCulloch CA, Szászi K, Mucsi I, Kapus A. Cell contact-dependent regulation of epithelial-myofibroblast transition via the rho-rho kinase-phospho-myosin pathway. *Mol Biol Cell.* 2007;18:1083-97.
22. Farkas A, Szatmári E, Orbók A, Wilhelm I, Wejksza K, Nagyoszi P, Hutamekalin P, Bauer H, Bauer HC, Traweger A, Krizbai IA. Hyperosmotic mannitol induces Src kinase-dependent phosphorylation of beta-catenin in cerebral endothelial cells. *J Neurosci Res.* 2005;80:855-61.
23. Fischer S, Wiesnet M, Marti HH, Renz D, Schaper W. Simultaneous activation of several second messengers in hypoxia-induced hyperpermeability of brain derived endothelial cells. *J Cell Physiol.* 2004;198:359-69.
24. Furuse M, Hirase T, Itoh M, Nagafuchi A, Yonemura S, Tsukita S, Tsukita S. Occludin: a novel integral membrane protein localizing at tight junctions. *J Cell Biol.* 1993;123:1777-88.
25. Furuse M, Fujita K, Hiiragi T, Fujimoto K, Tsukita S. Claudin-1 and -2: novel integral membrane proteins localizing at tight junctions with no sequence similarity to occludin. *J Cell Biol.* 1998;141:1539-50.
26. Gallicchio M, Mitola S, Valdembri D, Fantozzi R, Varnum B, Avanzi GC, Bussolino F. Inhibition of vascular endothelial growth factor receptor 2-mediated endothelial cell activation by Axl tyrosine kinase receptor. *Blood.* 2005;105:1970-6.
27. Gonzalez-Mariscal L, Contreras RG, Bolívar JJ, Ponce A, Chávez De Ramirez B, Cereijido M. Role of calcium in tight junction formation between epithelial cells. *Am J Physiol.* 1990;259:C978-86.

28. González-Mariscal L, Betanzos A, Nava P, Jaramillo BE. Tight junction proteins. *Prog Biophys Mol Biol.* 2003;81:1-44.
29. González-Mariscal L, Tapia R, Chamorro D. Crosstalk of tight junction components with signaling pathways. *Biochim Biophys Acta.* 2008;1778:729-56.
30. Gumbiner B, Lowenkopf T, Apatira D. Identification of a 160-kDa polypeptide that binds to the tight junction protein ZO-1. *Proc Natl Acad Sci U S A.* 1991;88:3460-4.
31. Hafizi S, Dahlbäck B. Gas6 and protein S. Vitamin K-dependent ligands for the Axl receptor tyrosine kinase subfamily. *FEBS J.* 2006(a);273:5231-44.
32. Hafizi S, Dahlbäck B. Signalling and functional diversity within the Axl subfamily of receptor tyrosine kinases. *Cytokine Growth Factor Rev.* 2006(b);17:295-304.
33. Harte MT, Hildebrand JD, Burnham MR, Bouton AH, Parsons JT. p130Cas, a substrate associated with v-Src and v-Crk, localizes to focal adhesions and binds to focal adhesion kinase. *J Biol Chem.* 1996;271:13649-55.
34. Hasanbasic I, Cuerquis J, Varnum B, Blostein MD. Intracellular signaling pathways involved in Gas6-Axl-mediated survival of endothelial cells. *Am J Physiol Heart Circ Physiol.* 2004;287:H1207-13.
35. Hawkins BT, Davis TP. The blood-brain barrier/neurovascular unit in health and disease. *Pharmacol Rev.* 2005;57:173-85.
36. Henderson E, Haydon PG, Sakaguchi DS. Actin filament dynamics in living glial cells imaged by atomic force microscopy. *Science.* 1992;257:1944-6.
37. Holland SJ, Powell MJ, Franci C, Chan EW, Frieria AM, Atchison RE, McLaughlin J, Swift SE, Pali ES, Yam G, Wong S, Lasaga J, Shen MR, Yu S, Xu W, Hitoshi Y, Bogenberger J, Nör JE, Payan DG, Lorens JB. Multiple roles for the receptor tyrosine kinase axl in tumor formation. *Cancer Res.* 2005;65:9294-303.
38. Hopkins AM, Walsh SV, Verkade P, Boquet P, Nusrat A. Constitutive activation of Rho proteins by CNF-1 influences tight junction structure and epithelial barrier function. *J Cell Sci.* 2003;116:725-42.
39. Hopkins AM, Pineda AA, Winfree LM, Brown GT, Laukoetter MG, Nusrat A. Organized migration of epithelial cells requires control of adhesion and protrusion through Rho kinase effectors. *Am J Physiol Gastrointest Liver Physiol.* 2007;292:G806-17.
40. Hubbard SR. Autoinhibitory mechanisms in receptor tyrosine kinases. *Front Biosci.* 2002;7:d330-40.
41. Itoh M, Nagafuchi A, Moroi S, Tsukita S. Involvement of ZO-1 in cadherin-based cell adhesion through its direct binding to alpha catenin and actin filaments. *J Cell Biol.* 1997;138:181-92.

42. Itoh M, Morita K, Tsukita S. Characterization of ZO-2 as a MAGUK family member associated with tight as well as adherens junctions with a binding affinity to occludin and alpha catenin. *J Biol Chem*. 1999;274:5981-6.
43. Ivanov AI, McCall IC, Parkos CA, Nusrat A. Role for actin filament turnover and a myosin II motor in cytoskeleton-driven disassembly of the epithelial apical junctional complex. *Mol Biol Cell*. 2004(a);15:2639-51.
44. Ivanov AI, Nusrat A, Parkos CA. Endocytosis of epithelial apical junctional proteins by a clathrin-mediated pathway into a unique storage compartment. *Mol Biol Cell*. 2004(b);15:176-88.
45. Kapus A, Szász K, Sun J, Rizoli S, Rotstein OD. Cell shrinkage regulates Src kinases and induces tyrosine phosphorylation of cortactin, independent of the osmotic regulation of Na⁺/H⁺ exchangers. *J Biol Chem*. 1999;274:8093-102.
46. Kilic E, Kilic U, Wang Y, Bassetti CL, Marti HH, Hermann DM. The phosphatidylinositol-3 kinase/Akt pathway mediates VEGF's neuroprotective activity and induces blood brain barrier permeability after focal cerebral ischemia. *FASEB J*. 2006;20:1185-7.
47. Korshunov VA, Mohan AM, Georger MA, Berk BC. Axl, a receptor tyrosine kinase, mediates flow-induced vascular remodeling. *Circ Res*. 2006;98:1446-52.
48. Korshunov VA, Daul M, Massett MP, Berk BC. Axl mediates vascular remodeling induced by deoxycorticosterone acetate-salt hypertension. *Hypertension*. 2007;50:1057-62.
49. Krizbai IA, Deli MA. Signalling pathways regulating the tight junction permeability in the blood-brain barrier. *Cell Mol Biol (Noisy-le-grand)*. 2003;49:23-31.
50. Kroll RA, Neuwelt EA. Outwitting the blood-brain barrier for therapeutic purposes: osmotic opening and other means. *Neurosurgery*. 1998;42:1083-99.
51. Lewis A, Di Ciano C, Rotstein OD, Kapus A. Osmotic stress activates Rac and Cdc42 in neutrophils: role in hypertonicity-induced actin polymerization. *Am J Physiol Cell Physiol*. 2002;282:C271-9.
52. Li B, Zhao WD, Tan ZM, Fang WG, Zhu L, Chen YH. Involvement of Rho/ROCK signalling in small cell lung cancer migration through human brain microvascular endothelial cells. *FEBS Lett*. 2006;580:4252-60.
53. Lok J, Sardi SP, Guo S, Besancon E, Ha DM, Rosell A, Kim WJ, Corfas G, Lo EH. Neuregulin-1 signaling in brain endothelial cells. *J Cereb Blood Flow Metab*. 2008.
54. Lunn JA, Rozengurt E. Hyperosmotic stress induces rapid focal adhesion kinase phosphorylation at tyrosines 397 and 577. Role of Src family kinases and Rho family GTPases. *J Biol Chem*. 2004;279:45266-78.
55. Ma TY, Tran D, Hoa N, Nguyen D, Merryfield M, Tarnawski A. Mechanism of extracellular calcium regulation of intestinal epithelial tight junction permeability: role of cytoskeletal involvement. *Microsc Res Tech*. 2000;51:156-68.

56. Mahajan SD, Aalinkeel R, Sykes DE, Reynolds JL, Bindukumar B, Adal A, Qi M, Toh J, Xu G, Prasad PN, Schwartz SA. Methamphetamine alters blood brain barrier permeability via the modulation of tight junction expression: Implication for HIV-1 neuropathogenesis in the context of drug abuse. *Brain Res.* 2008;1203:133-48.
57. Malek AM, Goss GG, Jiang L, Izumo S, Alper SL. Mannitol at clinical concentrations activates multiple signaling pathways and induces apoptosis in endothelial cells. *Stroke.* 1998;29:2631-40.
58. Martin-Padura I, Lostaglio S, Schneemann M, Williams L, Romano M, Fruscella P, Panzeri C, Stoppacciaro A, Ruco L, Villa A, Simmons D, Dejana E. Junctional adhesion molecule, a novel member of the immunoglobulin superfamily that distributes at intercellular junctions and modulates monocyte transmigration. *J Cell Biol.* 1998;142:117-27.
59. Meyer TN, Schwesinger C, Ye J, Denker BM, Nigam SK. Reassembly of the tight junction after oxidative stress depends on tyrosine kinase activity. *J Biol Chem.* 2001;276:22048-55.
60. Morita K, Sasaki H, Furuse M, Tsukita S. Endothelial claudin: claudin-5/TMVCF constitutes tight junction strands in endothelial cells. *J Cell Biol.* 1999;147:185-94.
61. O'Bryan JP, Fridell YW, Koski R, Varnum B, Liu ET. The transforming receptor tyrosine kinase, Axl, is post-translationally regulated by proteolytic cleavage. *J Biol Chem.* 1995;270:551-7.
62. Ohnishi H, Nakahara T, Furuse K, Sasaki H, Tsukita S, Furuse M. JACOP, a novel plaque protein localizing at the apical junctional complex with sequence similarity to cingulin. *J Biol Chem.* 2004;279:46014-22.
63. Ohtsuki S, Yamaguchi H, Katsukura Y, Asashima T, Terasaki T. mRNA expression levels of tight junction protein genes in mouse brain capillary endothelial cells highly purified by magnetic cell sorting. *J Neurochem.* 2008;104:147-54.
64. Park KW, Kwon YW, Cho HJ, Shin JI, Kim YJ, Lee SE, Youn SW, Lee HC, Kang HJ, Shaul PW, Oh BH, Park YB, Kim HS. G-CSF exerts dual effects on endothelial cells-Opposing actions of direct eNOS induction versus indirect CRP elevation. *J Mol Cell Cardiol.* 2008.
65. Perrière N, Demeuse P, Garcia E, Regina A, Debray M, Andreux JP, Couvreur P, Scherrmann JM, Tamsamani J, Couraud PO, Deli MA, Roux F. Puromycin-based purification of rat brain capillary endothelial cell cultures. Effect on the expression of blood-brain barrier-specific properties. *J Neurochem.* 2005;93:279-89.
66. Persidsky Y, Heilman D, Haorah J, Zelivyanskaya M, Persidsky R, Weber GA, Shimokawa H, Kaibuchi K, Ikezu T. Rho-mediated regulation of tight junctions during monocyte migration across the blood-brain barrier in HIV-1 encephalitis (HIVE). *Blood.* 2006(a);107:4770-80.

67. Persidsky Y, Ramirez SH, Haorah J, Kanmogne GD. Blood-brain barrier: structural components and function under physiologic and pathologic conditions. *J Neuroimmune Pharmacol.* 2006(b);1:223-36.
68. Pesen D, Hoh JH. Micromechanical architecture of the endothelial cell cortex. *Biophys J.* 2005;88:670-9.
69. Pitelka DR, Taggart BN, Hamamoto ST. Effects of extracellular calcium depletion on membrane topography and occluding junctions of mammary epithelial cells in culture. *J Cell Biol.* 1983;96:613-24.
70. Polte TR, Hanks SK. Interaction between focal adhesion kinase and Crk-associated tyrosine kinase substrate p130Cas. *Proc Natl Acad Sci U S A.* 1995;92:10678-82.
71. Ramirez SH, Heilman D, Morse B, Potula R, Haorah J, Persidsky Y. Activation of peroxisome proliferator-activated receptor gamma (PPARgamma) suppresses Rho GTPases in human brain microvascular endothelial cells and inhibits adhesion and transendothelial migration of HIV-1 infected monocytes. *J Immunol.* 2008;180:1854-65.
72. Rapoport SI. Advances in osmotic opening of the blood-brain barrier to enhance CNS chemotherapy. *Expert Opin Investig Drugs.* 2001;10:1809-18.
73. Rothen-Rutishauser B, Riesen FK, Braun A, Günthert M, Wunderli-Allenspach H. Dynamics of tight and adherens junctions under EGTA treatment. *J Membr Biol.* 2002;188:151-62.
74. Rotsch C, Radmacher M. Drug-induced changes of cytoskeletal structure and mechanics in fibroblasts: an atomic force microscopy study. *Biophys J.* 2000;78:520-35.
75. Schreibelt G, Kooij G, Reijerkerk A, van Doorn R, Gringhuis SI, van der Pol S, Weksler BB, Romero IA, Couraud PO, Piontek J, Blasig IE, Dijkstra CD, Ronken E, de Vries HE. Reactive oxygen species alter brain endothelial tight junction dynamics via RhoA, PI3 kinase, and PKB signaling. *FASEB J.* 2007;21:3666-76.
76. Schrot S, Weidenfeller C, Schäffer TE, Robenek H, Galla HJ. Influence of hydrocortisone on the mechanical properties of the cerebral endothelium in vitro. *Biophys J.* 2005;89:3904-10.
77. Schulze C, Firth JA. Immunohistochemical localization of adherens junction components in blood-brain barrier microvessels of the rat. *J Cell Sci.* 1993;104:773-82.
78. Siegal T, Rubinstein R, Bokstein F, Schwartz A, Lossos A, Shalom E, Chisin R, Gomori JM. In vivo assessment of the window of barrier opening after osmotic blood-brain barrier disruption in humans. *J Neurosurg.* 2000;92:599-605.
79. Staddon JM, Herrenknecht K, Smales C, Rubin LL. Evidence that tyrosine phosphorylation may increase tight junction permeability. *J Cell Sci.* 1995;108:609-19.
80. Stamatovic SM, Keep RF, Kunkel SL, Andjelkovic AV. Potential role of MCP-1 in endothelial cell tight junction 'opening': signaling via Rho and Rho kinase. *J Cell Sci.* 2003;116:4615-28.

81. Stamatovic SM, Dimitrijevic OB, Keep RF, Andjelkovic AV. Protein kinase Calpha-RhoA cross-talk in CCL2-induced alterations in brain endothelial permeability. *J Biol Chem.* 2006;281:8379-88.
82. Stevenson BR, Siliciano JD, Mooseker MS, Goodenough DA. Identification of ZO-1: a high molecular weight polypeptide associated with the tight junction (zonula occludens) in a variety of epithelia. *J Cell Biol.* 1986;103:755-66.
83. Tai KY, Shieh YS, Lee CS, Shiah SG, Wu CW. Axl promotes cell invasion by inducing MMP-9 activity through activation of NF-kappaB and Brg-1. *Oncogene.* 2008;27:4044-55.
84. Ueno E, Haruta T, Uno T, Usui I, Iwata M, Takano A, Kawahara J, Sasaoka T, Ishibashi O, Kobayashi M. Potential role of Gab1 and phospholipase C-gamma in osmotic shock-induced glucose uptake in 3T3-L1 adipocytes. *Horm Metab Res.* 2001;33:402-6.
85. Vajkoczy P, Knyazev P, Kunkel A, Capelle HH, Behrndt S, von Tengg-Kobligk H, Kiessling F, Eichelsbacher U, Essig M, Read TA, Erber R, Ullrich A. Dominant-negative inhibition of the Axl receptor tyrosine kinase suppresses brain tumor cell growth and invasion and prolongs survival. *Proc Natl Acad Sci U S A.* 2006;103:5799-804.
86. Vogel C, Bauer A, Wiesnet M, Preissner KT, Schaper W, Marti HH, Fischer S. Flt-1, but not Flk-1 mediates hyperpermeability through activation of the PI3-K/Akt pathway. *J Cell Physiol.* 2007;212:236-43.
87. Weinger JG, Gohari P, Yan Y, Backer JM, Varnum B, Shafit-Zagardo B. In brain, Axl recruits Grb2 and the p85 regulatory subunit of PI3 kinase; in vitro mutagenesis defines the requisite binding sites for downstream Akt activation. *J Neurochem.* 2008;106:134-46.
88. Weksler BB, Subileau EA, Perrière N, Charneau P, Holloway K, Leveque M, Tricoire-Leignel H, Nicotra A, Bourdoulous S, Turowski P, Male DK, Roux F, Greenwood J, Romero IA, Couraud PO. Blood-brain barrier-specific properties of a human adult brain endothelial cell line. *FASEB J.* 2005;19:1872-4.
89. Yamamoto M, Ramirez SH, Sato S, Kiyota T, Cerny RL, Kaibuchi K, Persidsky Y, Ikezu T. Phosphorylation of claudin-5 and occludin by rho kinase in brain endothelial cells. *Am J Pathol.* 2008;172:521-33.
90. Zhang Y, Park TS, Gidday JM. Hypoxic preconditioning protects human brain endothelium from ischemic apoptosis by Akt-dependent survivin activation. *Am J Physiol Heart Circ Physiol.* 2007;292:H2573-81.

7. ACKNOWLEDGEMENTS

I would like to express my warmest gratitude to Dr. István Krizbai for his scientific guidance, encouragement and support throughout my Ph.D. studies.

I express my thanks to Dr. Árpád Párducz, the previous and Dr. László Siklós, the present head of the Laboratory of Molecular Neurobiology, and to all my colleagues in the group and in the Biological Research Center.

I am extremely grateful to the team of the brain endothelial research subgroup (Attila E. Farkas, Péter Nagyőszzi, Csilla Fazakas) for all the time that we have spent together inside and outside the laboratory. Many thanks to the previous members Anna Orbók and Pilaiwanwadee Hutamekalin and to Ngo Thi Khue Dung for her excellent technical assistance. I would like to thank Dr. György Váró and his co-workers for the atomic force microscopy studies.

I am very grateful to all the people who have supported me before and during my Ph.D. work, including teachers, colleagues and friends, even if not mentioned here by name. I would like to thank István for standing by me all the time. I am especially thankful to my family for their support and love during my whole life.

8. APPENDIX

I. Wilhelm I, Nagyőszzi P, Farkas AE, Couraud PO, Romero IA, Weksler B, Fazakas C, Dung NT, Bottka S, Bauer H, Bauer HC, Krizbai IA. Hyperosmotic stress induces Axl activation and cleavage in cerebral endothelial cells. *J Neurochem.* 2008, **107**:116-26.

II. Wilhelm I, Farkas AE, Nagyőszzi P, Váró G, Bálint Z, Végh GA, Couraud PO, Romero IA, Weksler B, Krizbai IA. Regulation of cerebral endothelial cell morphology by extracellular calcium. *Phys Med Biol.* 2007, **52**:6261-74.